GENIORS

Research and Innovation Action (RIA)

This project has received funding from the European Union's Horizon 2020 research and innovation programme under grant agreement No 755171.

Start date : 2017-06-01 Duration : 48 Months
http://geniors.eu/

Status on TODGAorganic phase loading

Authors : Mr. Andreas GEIST (KIT), A. Paquet (CEA), G. Saint-Louis (CEA), L. Berthon (CEA), P. Guilbaud (CEA), P. Wessling (KIT), T. Sittel (KIT), P. J. Panak (KIT), A. Geist (KIT)

GENIORS - Contract Number: 755171

Project officer: Roger Garbil

Document title	Status on TODGAorganic phase loading
Author(s)	Mr. Andreas GEIST, A. Paquet (CEA), G. Saint-Louis (CEA), L. Berthon (CEA), P. Guilbaud (CEA), P. Wessling (KIT), T. Sittel (KIT), P. J. Panak (KIT), A. Geist (KIT)
Number of pages	43
Document type	Deliverable
Work Package	WP3
Document number	D3.3
Issued by	KIT
Date of completion	2020-05-13 17:20:44
Dissemination level	Public

Summary

Deliverable D3.3 Status on TODGA organic phase loading reports studies on the aggregation of diglycolamide (DGA) extractants and on their Ln(III) and Pd(IV) loading behaviour. The first part of the deliverable is dedicated to understand the aggregation of species in the solution (metals, extractant and modifiers), since it is directly is correlated to the third phase formation. In this study, performed by CEA, a methodology has been applied coupling experimental and theoretical methods. The composition of the organic phase has been determined experimentally and used to build molecular dynamics simulation boxes with the same composition as the experimental solutions. Results indicate that at the modifiers concentrations used of in the i-SANEX and EURO-GANEX processes, the TODGA extractant remains in the cation first coordination sphere preserving its significant role in the complexation/selectivity of the cations, but both modifiers studied have a significant role in the speciation of these cations in the organic phase. The second part of this deliverable is dedicated to a study performed by KIT regarding the extraction of Ln(III) and Pu(IV) into various diglycolamide (DGA) based solvents under loading conditions, such as the reference EURO-GANEX solvent and two alternative solvents (TODGA in DIPB and cis-mTDDGA in Exxsol D80). Results show the formation of 1:3 complexes, [M(TODGA)3]3+ under non-loading conditions for Ln(III); however, at loading conditions, the formation of a 1:2 TODGA complex was identified, which must be accounted for in equilibrium models. The TODGA in DIPB solvent proposed is not useful for EURO-GANEX applications due to its insufficient Pu loading capacity, in contrast to the promising results obtained for the cis-mTDDGA solvent.

Approval

Date	By
2020-05-13 17:54:32	Mr. Philippe GUILBAUD (CEA)
2020-05-14 08:20:53	Mr. Andreas GEIST (KIT)
2020-05-19 08:03:57	Mr. Stéphane BOURG (CEA)

CONTENT

This project has received funding from the EURATOM research and training programme 2014–2018 under grant agreement No 730227

EXECUTIVE SUMMARY

Deliverable D3.3 *Status on TODGA organic phase loading* reports studies on the aggregation of diglycolamide (DGA) extractants and on their Ln(III) and Pu(IV) loading behaviour.

The first part of the deliverable is dedicated to understanding the aggregation of species in the solution (metals, extractant and modifiers), since it is directly is correlated to the third phase formation. In this study, performed by CEA, a methodology has been applied coupling experimental and theoretical methods. The composition of the organic phase has been determined experimentally and used to build molecular dynamics simulation boxes with the same composition as the experimental solutions. Results indicate that at the modifiers concentrations used of in the *i*-SANEX and EURO-GANEX processes, the TODGA extractant remains in the cation first coordination sphere preserving its significant role in the complexation/selectivity of the cations, but both modifiers studied have a significant role in the speciation of these cations in the organic phase.

The second part of this deliverable is dedicated to a study performed by KIT regarding the extraction of Ln(III) and Pu(IV) into various diglycolamide (DGA) based solvents under loading conditions, such as the reference EURO-GANEX solvent and two alternative solvents (TODGA in DIPB and *cis*-mTDDGA in Exxsol D80). Results show the formation of 1:3 complexes, $[M(TODGA)_3]^{3+}$ under non-loading conditions for Ln(III); however, at loading conditions, the formation of a 1:2 TODGA complex was identified, which must be accounted for in equilibrium models. The TODGA in DIPB solvent proposed is not useful for EURO-GANEX applications due to its insufficient Pu loading capacity, in contrast to the promising results obtained for the *cis*-mTDDGA solvent.

This project has received funding from the EURATOM research and training programme 2014–2018 under grant agreement No 730227

ORGANIZATION OF TODGA BASED SOLVENT EXTRACTION SOLUTIONS

CEA: A. Paquet, G. Saint-Louis, L. Berthon, P. Guilbaud

INTRODUCTION

TODGA has been evaluated extensively for actinides partitioning and experienced even with genuine nuclear waste solution.[1] One disadvantage of this extractant family is its limited loading capacity without third phase formation in alkane, *i.e.* the maximum concentration of metal ions or acid that can be loaded in the organic phase. Typically, a third phase (i.e. the splitting of the organic phase into two phases) is observed when 0.2M TODGA in *n*-dodecane is contacted with 4M HNO_3 or, when 0.2M TODGA in TPH is contacted with 0.1M $Nd(NO_3)_3$ in 5M nitric acid.[2-7] Although the maximum solute concentration in the organic phase or the limiting organic concentration (LOC) increases with the TODGA concentration and the temperature, phase modifiers are frequently introduced into the solvent to use this molecule in actual solvent extraction processes. In a recent review, Whittaker et al. present the current state of knowledge regarding the application of DGA extractants in minor actinides separation processes, focusing specially on the use of modifiers.[8]

An option to suppress the third phase consist in replacing n-dodecane by pure 1-octanol[2] or adding 5% of *n*-octanol in the organic phase.[3] Thus, in the innovative-SANEX process developed in the frame of several European project, the solvent consists of 0.2M TODGA + 5% 1-octanol in TPH.[3, 9-12] Finally, DMDOHEMA which is used as the extractant for the DIAMEX-SANEX process[13] was also tested to increase the loading capacity of the TODGA-based processes: the combination of 0.2M TODGA and 0.5M DMDOHEMA in kerosene was selected as the most suitable organic phase composition for the second cycle of the EURO-GANEX process.[14-18]

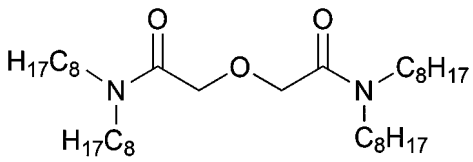

Figure 1. Molecular structure of TODGA.

It is important to emphasize that for all these processes, the concentration of the 'phase modifier' or 'co-extractant' in the organic phase is significant (for example 5% of octanol in dodecane solution represents 0.32M, a higher concentration than the TODGA concentration) and that this could induce changes in the speciation at both the molecular and the supramolecular scale.

At the molecular scale, several stoichiometries from 1:2 to 1:4 metal(III):TODGA complexes are reported in the literature. Most of these stoichiometries are derived from solvent extraction slope analysis data. Some authors propose the 1:2 stoichiometry for metal(III):TODGA complex in polar diluents[19-21] and a 1:3 (or 1:4) stoichiometry in non-polar diluents.[2-3, 20-26] The metal(III):TODGA complexes were characterized by spectroscopy techniques and DFT calculation.[27] TRLFS studies on

This project has received funding from the EURATOM research and training programme 2014–2018 under grant agreement No 730227

Eu(III)-TODGA-diluent-HNO_3 revealed that the inner coordination sphere of Eu was totally dehydrated whatever the diluent used: dodecane, toluene, octanol or even in presence of 0.5M DHOA. [25, 28-29] EXAFS measurements of TODGA in isododecanol-alkane after lanthanides extraction suggest the presence of $[Ln(DGA)_3]^{3+}$ with tridentate DGAs.[26, 30] IR spectroscopy confirm that the carbonyl group of the amide function coordinate the lanthanide cations[20, 24] whereas the coordination of the ether function is less clear.

On the other hand, it is now well known that the third phase formation is correlated to the aggregation of species in the solution.[31] The aggregation of TODGA in organic solution were investigated by vapor pressure osmometry, small angle X ray, small angle neutrons scattering and dynamic light scattering analyses.[6, 19, 32-35] TODGA in aliphatic diluent solutions after contact with aqueous phases (nitric acid with and without neodymium salts) are composed of polydisperse mixture containing monomers, dimers and small reverse micelles of TODGA tetramers. They respective proportions depend on the TODGA concentration, the nature and concentration of extracted solutes as well as the nature of the diluent.[6, 19, 32-35] Some study of the aggregation of TODGA in n-dodecane with 0.5 M DHOA or 5% of 1-octanol revealed that the size of the aggregate is bigger in presence of 1-octanol than in presence of DHOA.[35] When *n*-dodecane is replaced by pure 1-octanol, no TODGA aggregate are observed in solution.[19] Some molecular dynamic simulation were performed for TODGA solution in dodecane containing water, nitric acid or lanthanide nitrate[27, 36-37] but none of these studies took into account concentration effects on the speciation.

In this study, we applied the method coupling experimental and theoretical characterization already used for the description of organic solutions in several solvent extraction system.[38-41] The composition of the organic phase is determined experimentally and used to build molecular dynamics simulation boxes with the same composition as the experimental solutions. The representativeness of the simulation is then checked by comparing experimental data (densities and both small and wide angle X-ray scattered intensities) with the calculated one.

RESULTS

WATER EXTRACTION

Organic phases containing either TODGA 0.2M alone, TODGA 0.2M + 5% (0.32M) octanol, or TOGDA 0.2M + DMDOHEMA 0.5M in n-heptane have been contacted with pure water in order to assess the speciation and extractants organization in these solutions. After equilibration, the amount of water in the organic phase has been determined. The composition of the resulting experimental organic phase is reported in Table 1 (left). The presence of 0.32M octanol in the organic phase leads to a slight increase in the water concentration (0.08 vs. 0.06). The presence of 0.5M DMDOHEMA leads to a significant increase in the water concentration. It is well known that DMDOHEMA in alkane extract significant quantity of water: 0.15M of water is extracted by 0.5M DMDOHEMA in *n*-heptane.[42]The quantity of water extracted by 0.2M TODGA + 0.5M DMDOHEMA solution is a slightly higher than the addition of the concentration extracted by the solutions of the single extractant (0.25 vs 0.21M). It is

This project has received funding from the EURATOM research and training programme 2014–2018 under grant agreement No 730227

likely that this slight increase in the concentration of water is due to a higher organization of the species in the organic phase.

The presence of interactions between species has first been checked by ESI-MS analysis. As reported in the literature, the structural organization of surfactants in the gas phase is considered to depend on the nature and composition of the starting solution.[43] Previous analysis of organic phases by ESI-MS shown consistency between the species identified in the mass spectra and the adducts or complexes existing in the solution.[13, 41, 44-48] The Figure 2 reports the ESI-MS spectra in positive ionization mode corresponding to organic solutions after contact with water. The assignment of the main species is presented in Table 2. The analysis of the solution of TODGA 0.2M in n-heptane indicate the presence of ions containing 1 to 5 TODGA molecules, indicating the possible presence of aggregate containing up to 5 TODGA molecules in the organic phase. For organic solution containing 0.32M of octanol, no species containing octanol molecules are observed. It is worth noting that the interaction between octanol and other species are very low and that octanol molecules are very volatile. This does not mean therefore that octanol molecules are excluded from the aggregates in the solution. Moreover, ions containing several TODGA molecules are less abundant suggesting a decrease of the interaction between TODGA molecules. For solution containing 0.2M TODGA + 0.5M DMDOHEMA, DMDOHEMA and TODGA species containing 1 to 2 molecules are formed as well as mixed species involving the two ligands. Even if these information's are only qualitative, this shows that the speciation in the organic phase (adducts or aggregates distribution) depends strongly on the composition of the solutions.

Table 1. Composition of the experimental solutions (left) and corresponding number of molecules in the MD simulation (right) (T is TODGA and D is DMDOHEMA).

Concentration (M)		ρ_{exp}	ρ_{calc}	Number of molecules in the simulation				
ligands	H_2O	(g/cm^3)	(g/cm^3)	heptane	T	D	octanol	H_2O
TODGA 0.2	0.06	0.717	0.712	3000	106	0	0	30
TODGA 0.2 + 5% octanol	0.08	0.722	0.715	2750	94	0	144	41
TODGA 0.2 + DMDOHEMA 0.5	0.25	0.781	0.782	2000	100	245	0	122

This project has received funding from the EURATOM research and training programme 2014–2018 under grant agreement No 730227

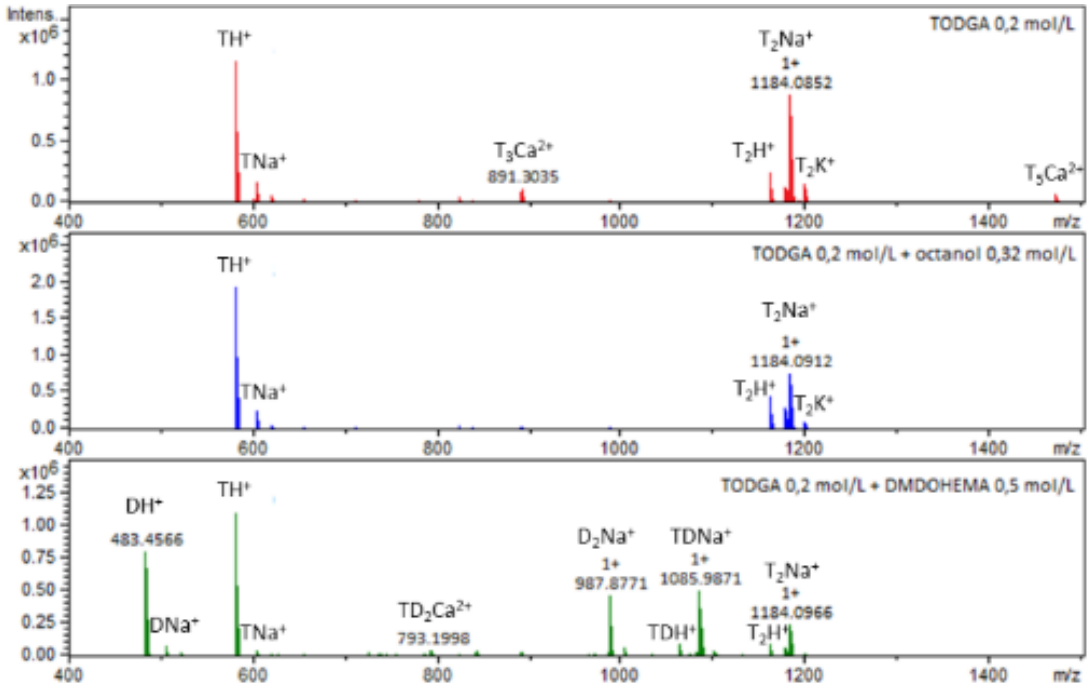

Figure 2. ESI-MS spectra of the organic phases after contact with pure water. TODGA 0.2M (top), TODGA 0.2M + 5% octanol (center) and TODGA 0.2M + DMDOHEMA 0.5M (bottom). Dilution x10000 in CH_3CN/water (50%/50%).

Table 2. m/z ratios and assignments of the main ions detected by ESI-MS for solutions of TODGA 0.2M in n-heptane, TODGA 0. 2M + 5% octanol in n-heptane, and TODGA 0.2M + DMDOHEMA 0.5M in n-heptane (T = TODGA and D = DMDOHEMA).

m/z			Assignment
TODGA	TODGA Octanol	TODGA DMDOHEMA	
/	/	483.4	DH^+
/	/	505.4	DNa^+
/	/	521.4	DK^+
581.6	581.6	581.6	TH^+
603.5	603.5	603.5	TNa^+
619.5	619.5	619.5	TK^+
/	/	792.7	TD_2Ca^{2+}
890.8	/	/	T_3Ca^{2+}
/	/	987.9	D_2Na^+
/	/	1003.8	D_2K^+
/	/	1064.4	TDH^+
/	/	1085.4	$TDNa^+$
1162.1	1162.1	1162.1	T_2H^+
1181	/	/	T_4Ca^{2+}
1184.1	1184.1	1184.1	T_2Na^+
1200.1	1200.1	/	T_2K^+
1471.3	/	/	T_5Ca^{2+}

This project has received funding from the EURATOM research and training programme 2014–2018 under grant agreement No 730227

To obtain a comprehensive analysis of the organization of such organic solutions, Small and W ide Angle X-ray Scattering (SWAXS) measurements have been performed (see Figure 3 left).

Molecular dynamic (MD) simulations have also been performed for theoretical solution with precisely the same composition than the experimental ones (Table 1 and Figure 4): MD simulations boxes were built with molecule amounts calculated from the experimentally obtained composition and molecules initially randomly distributed. The acceptability of the structure obtained with the MD simulations is checked by comparing experimental data like the solution density and the SWAXS signal with the calculated ones (Table 1 and Figure 3). Then a complete analysis of the MD simulated organic phase allows us to characterize the structure in the solutions both at the molecular and supramolecular scales.

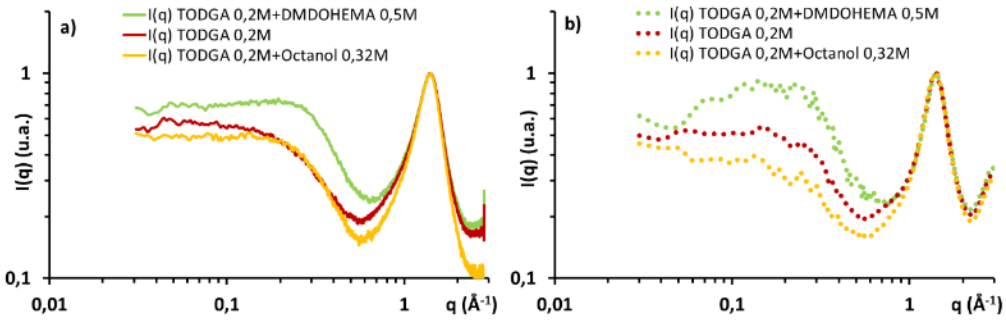

Figure 3. Experimental (a) and calculated (b) SWAXS signals for the organic phases after contact with pure water.

This project has received funding from the EURATOM research and training programme 2014–2018 under grant agreement No 730227

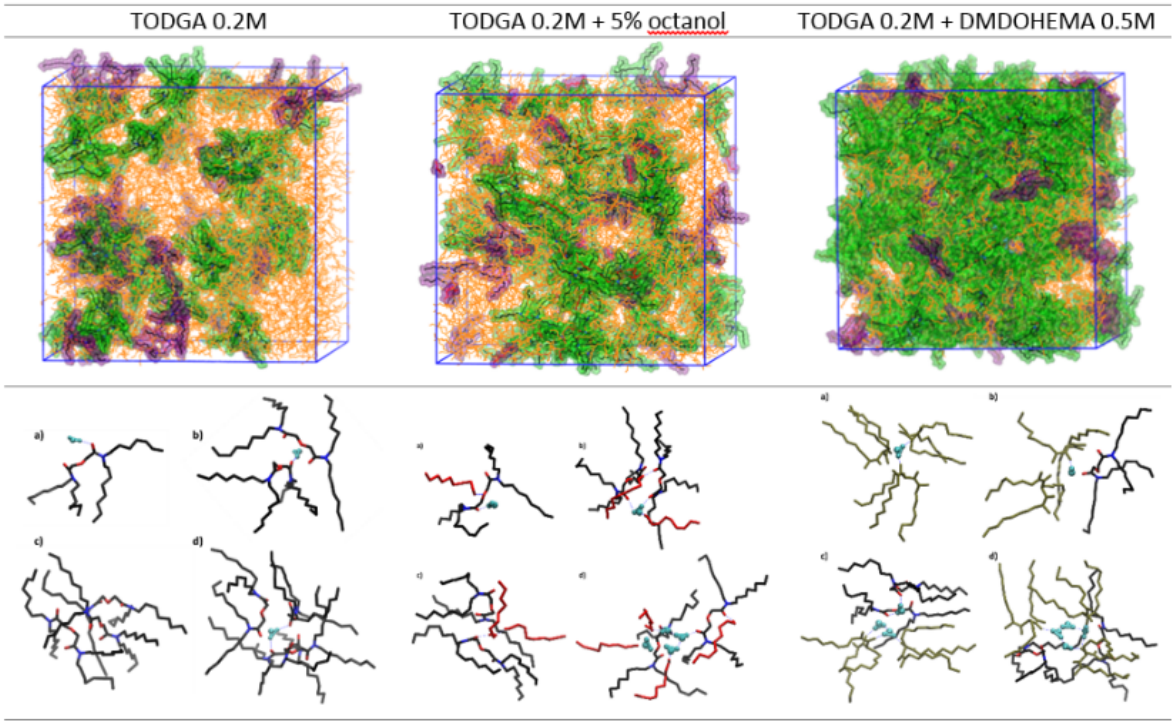

Figure 4. Snapshots of the MD simulation boxes (up) and corresponding typical aggregates (bottom) after extraction of water. Diluent molecules are in orange, extractant monomers are highlighted in purple, and aggregates are highlighted in green.

In the organic phase containing TODGA only, 26% of the TODGA molecules are monomers. The 74% remaining form small labile aggregates containing mainly 2 to 3 TODGA molecules with a very low amount of water molecules in these aggregates. Adding 5% octanol (0.32M) leads to (i) a small increase of the amount of water in the organic phase ([H_2O] ranges from 0.06 to 0.085M), (ii) a decrease of the aggregation state of the solution (40% of the TODGA molecules are monomers), and (iii) the formation of mixed aggregates that contain 1 to 3 TODGA and 1 to 4 octanol molecules. These mixed aggregates solvate more water than the aggregates formed with TODGA only.

In the organic phases containing 0.2M TODGA and 0.5M DMDOHEMA, the DMDOHEMA extractants drive the organization: each aggregate contains at least one DMODHEMA, and none of the aggregates is formed with TODGA only. Some aggregates containing only DMDOHEMA are observed. The amount of water in these TODGA+DMDOHEMA organic phase is much higher ([H_2O] = 0.25M) than in the solution that contain TODGA only, this results in the presence of water molecules in most of the aggregates. These observations, issuing from the analyses of the MD simulation trajectories is consistent with the evolution of the experimental SWAXS signals and in good agreement with the ESI-MS results.

NEODYNIUM NITRATE EXTRACTION

Organic phases (TODGA 0.2M alone, TODGA 0.2M + 5% vol. (i.e. 0.32M) octanol, or TOGDA 0.2M + DMDOHEMA 0.5M in n-heptane) have been contacted with aqueous phases containing different concentration of neodymium nitrate in order to assess the influence of the neodymium salt loading on

This project has received funding from the EURATOM research and training programme 2014–2018 under grant agreement No 730227

the structure of the complexes and aggregates formed in the organic phases. Each organic phase has been characterized using FT-IR spectroscopy, ESI-MS spectrometry, Small and Wide Angle X-ray Scattering (SWAXS) and molecular dynamic simulations. The compositions of the studied organic phases are reported in Table 3. In order to compare the different solutions, the initial $Nd(NO_3)_3$ aqueous concentrations (before extraction) have been chosen in order to obtain a comparable $Nd(NO_3)_3$ concentration after extraction in the organic phase (around 0.06M). This concentration corresponds to the maximum neodymium concentration in the organic phase before third phase formation for the 0.2M TODGA solution in n-heptane. In presence of 5% of octanol, or 0.5M DMDOHEMA, this value is increased. As indicated in Table 3, the coextracted water concentration in the organic phase increases with the neodymium extraction, about 1 to 2 water molecules per neodymium molecule.

Table 3. Composition of the studied experimental solutions (left) and corresponding number of molecules in the MD simulation (right) (T is TODGA and D is DMDOHEMA). Values in bracket correspond to the extracted water concentration when organic phases are contacted with water only.

	Experiments			**Simulations**						
	Concentration (M)				Number of molecules					
	$Nd(NO_3)_3$	H_2O	ρ_{exp} (g/cm³)	ρ_{calc} (g/cm³)	heptane	T	D	Oct	$Nd(NO_3)_3$	H_2O
TODGA 0.2M	0.019	0.08 (0.06)	0.720	0.714	2750	93	0	0	9	38
	0.059	0.15 (0.06)	0.731	0.728	2500	86	0	0	25	64
TODGA 0.2M + 5% Octanol	0.063	0.21 (0.08)	0.739	0.733	2750	94	0	144	31	41
	0.079	0.21 (0.08)	0.744	0.738	2750	94	0	144	39	41
TODGA 0.2M + DMDOHEMA 0.5M	0.059	0.38 (0.25)	0.798	0.798	2000	99	245	0	29	185
	0.093	0.41 (0.25)	0.809	0.807	2200	109	270	0	50	220

INFRARED AND UV-VISIBLE SPECTROSCOPIES

Infrared spectra of the organic phases before and after extraction of neodymium nitrate are reported in Figure 5. The first relevant vibration band to look at is the one corresponding to the amide C=O organic function. For the three solutions (organic phases containing TODGA only, TODGA + 5% octanol, or TODGA + DMDOHEMA), the absorbance of the free C=O vibration band at 1652 cm^{-1} decreases after nitrate neodymium extraction in the organic phase and a vibration band corresponding to a bonded C=O bond appears at 1616 cm^{-1}. The location of this bonded C=O vibration band is the same for the three organic phases indicating that the interaction between the amide function and the Nd^{3+} cation is similar in all cases as previously observed by Sasaki et al.[20, 24]

For the two first solutions (TODGA only, and TODGA + 5% octanol), the ether C-O-C vibration band is only slightly moved (from 1126 to 1122 cm^{-1}) after $Nd(NO_3)_3$ extraction indicating a very small interaction between Nd^{3+} and the ether function of the TODGA extractant, in agreement with Sasaki's results.[20] For the last organic phase (TODGA 0.2M + DMDOHEMA 0.5M), the C-O-C vibration band is

This project has received funding from the EURATOM research and training programme 2014–2018 under grant agreement No 730227

located at 1114 cm^{-1} and is not moved upon neodymium nitrate extraction. In this last case, this vibration band is mainly due to the DMDOHEMA that is at a concentration more than twice higher than the TODGA concentration. This is in agreement with previous studies on DMDOHEMA alone that show that the ether bond does not bind the lanthanide cations.

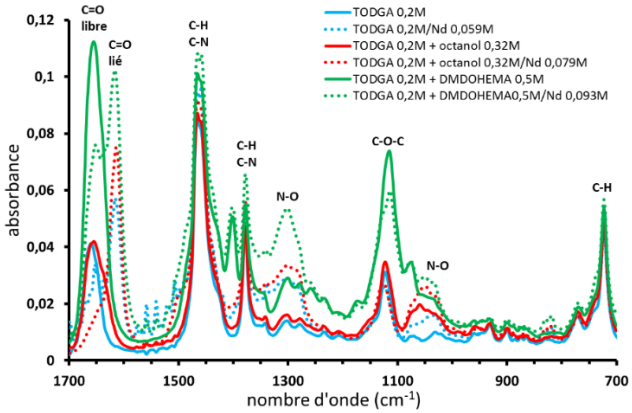

Figure 5. Infrared spectra of the TODGA solutions before and after extraction of neodymium nitrate. Blue: TODGA 0.2M in heptane, red: TODGA 0.2M + 5% octanol in heptane and green: TODGA 0.2M + DMDOHEMA 0.5M in heptane. Plain lines: solutions before neodymium extraction – dashed lines: solutions after neodymium extraction.

UV-visible spectroscopy was used to explore the neodymium environment after extraction for each solution (Figure 6). A change in the coordination sphere of the cation should induce a change in the absorption band. [49-51] The similarity of the spectra obtained after extraction of about 0.06M Nd for each of these 3 solutions with or without octanol or DMDOHEMA (Figure 6) shows that the immediate surrounding of the neodymium cations does not drastically change. It is possible that octanol molecules or DMDOHEMA molecule replace water or TODGA molecule around the metallic cation without changing the strength of the interactions.

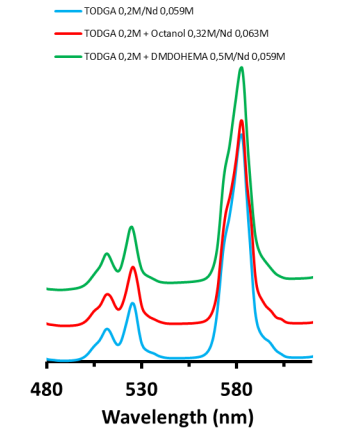

Figure 6. UV-visible spectra of the TODGA solutions after extraction of about 0.06M neodymium nitrate. Blue: TODGA 0.2M in heptane, red: TODGA 0.2M + 5% octanol in heptane and green: TODGA 0.2M + DMDOHEMA 0.5M in heptane.

This project has received funding from the EURATOM research and training programme 2014–2018 under grant agreement No 730227

ESI-MS ANALYSIS

The Figure 7 reports the ESI-MS spectra in positive ionization mode corresponding to the organic solutions after neodymium extraction. The assignment of the main species is presented in Table 4. After extraction of $Nd(NO_3)_3$ in the 0.2M TODGA organic phase, ions containing Nd^{3+} surrounded by 3 to 5 TODGA are observed on ESI-MS spectra (Figure 7a). In the organic phases with 5% octanol, the number of TODGA surrounding the Nd^{3+} cations decreases: 2 to 4 TODGA only, with a very low intensity for the species with 4 TODGA (Figure 7b). As for experiments without metallic cation, octanol molecules are not observed on these spectra but the decrease number of TODGA extractants around Nd^{3+} suggests that some octanol molecules may have replaced some TODGA around the cation in the solution. For the TODGA-DMDOHEMA organic phase (Figure 7c), Nd^{3+} is located in mixed aggregates (i.e. containing both TODGA and DMDOHEMA extractants), or in complexes or aggregates containing either TODGA or DMDOHEMA. All these species intensities are very low on the ESI-MS spectra due to the high polydispersity of the species observed.

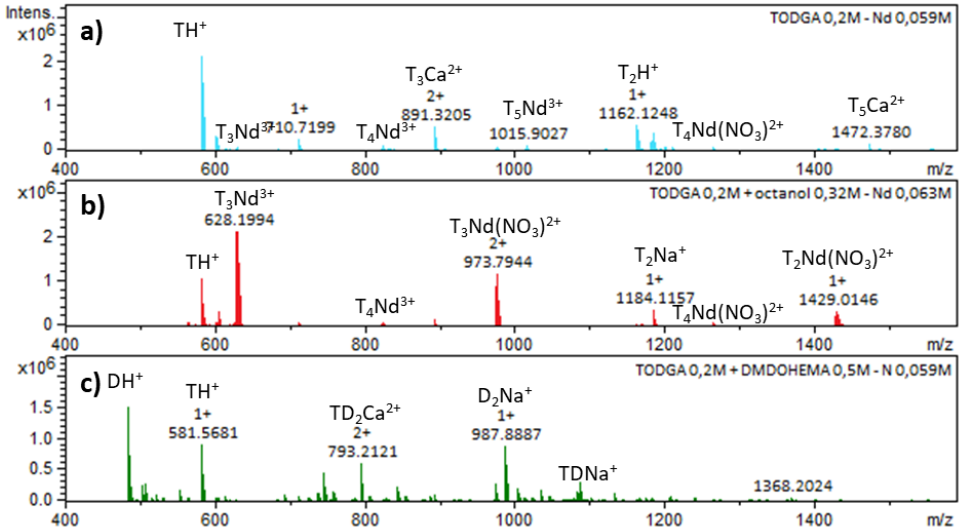

Figure 7. ESI-MS spectra of the solutions: TODGA 0.2M (a), TODGA 0.2M + 5% octanol (b) and TODGA 0.2M + DMDOHEMA 0.5M (c) in n-heptane after extraction of about 0.06 mol/L neodymium nitrate. Dilution 10000 in CH_3CN/water 50%/50%, isCID OeV.

Table 4. m/z ratios and assignments of the main ions detected by ESI-MS for solutions of TODGA 0.2M in n-heptane, TODGA 0.2M in n-heptane + 5% 1-octanol, and TODGA 0.2M + DMDOHEMA 0.5M in n-heptane after neodymium nitrate extraction. T = TODGA and D = DMDOHEMA. Ions containing Nd^{3+} are in bold and * indicates that the abundance of the species are very low.

m/z			
TODGA	**TODGA Octanol**	**TODGA DMDOHEMA**	**Assigments**
/	/	483,4	DH^+
/	/	502,4	D_2Ca^{2+}
/	/	505,4	DNa^+
/	/	**529,7***	**D_3Nd3^+**
581,6	581,6	581,6	TH^+

TODGA	m/z TODGA Octanol	TODGA DMDOHEMA	Assigments
600,5	/	/	T_2Ca^{2+}
603,5	603,5	603,5	TNa^{+}
627,8	**627,8**	**/**	**T_3Nd^{3+}**
/	/	**691,6***	**D_4Nd^{3+}**
/	/	**723,8***	**D_3TNd^{3+}**
/	/	743,7	D_3Ca^{2+}
/	/	792,7	D_2TCa^{2+}
821,3	**821,3**	**/**	**T_4Nd^{3+}**
/	/	**825,6***	**$D_3Nd(NO_3)^{2+}$**
/	/	**851,3***	**D_5Nd^{3+}**
/	/	**885,6***	**D_4TNd^{3+}**
890,8	890,8	890,8	T_3Ca^{2+}
/	/	**917,8***	**$D_3T_2Nd^{3+}$**
/	/	**923,7***	**$DT_2Nd(NO_3)^{2+}$**
972,8	**972,8**	**972,8***	**$T_3Nd(NO_3)^{2+}$**
/	/	987,9	D_2Na^{+}
/	/	**1012,2***	**D_6Nd^{3+}**
1015,9	**/**	**/**	**T_5Nd^{3+}**
/	/	**1046,9***	**D_5TNd^{3+}**
/	/	**1066,8***	**$D_4Nd(NO_3)^{2+}$**
/	/	1085,4	$DTNa^{+}$
1162,1	/	/	T_2H^{+}
/	/	**1173,0***	**D_7Nd^{3+}**
1184,1	1184,1	1184,1	T_2Na^{+}
/	/	**1207***	**D_6TNd^{3+}**
/	**/**	**1230,7***	**$D_2Nd(NO_3)_2^{+}$**
1263,1	**1263,1**	**1263,1***	**$T_4Nd(NO_3)^{2+}$**
/	**/**	**1308,1***	**$D_5Nd(NO_3)^{2+}$**
/	**1428,0**	**/**	**$T_2Nd(NO_3)_2^{+}$**
1471,3	/	/	T_5Ca^{2+}

SMALL AND WIDE ANGLE X-RAY SCATTERING

The experimental SWAXS intensities of the organic phases loaded with $Nd(NO_3)_3$ are reported on Figure 8. In all cases a "solvent pic" corresponding to the carbon-carbon interactions is observed at 1.42 $Å^{-1}$. The shape and the intensities of the SWAXS signal toward the smaller angles differs upon the composition of the organic phase.

For the TODGA 0.2M organic phases (blue curves on Figure 8), only a slight small angle signal increase is observed at low (0.02M) $Nd(NO_3)_3$ concentration, while an important increase is observed at 0.06M $Nd(NO_3)_3$. It is worth noting that the latest solution is very close to the cation saturation (i.e. just before segregation of the organic phase). The shape of these SWAXS intensities suggest the formation of small complexes or aggregates at low neodymium concentration and the formation of large (or numerous) aggregates at higher neodymium concentration.

This project has received funding from the EURATOM research and training programme 2014–2018 under grant agreement No 730227

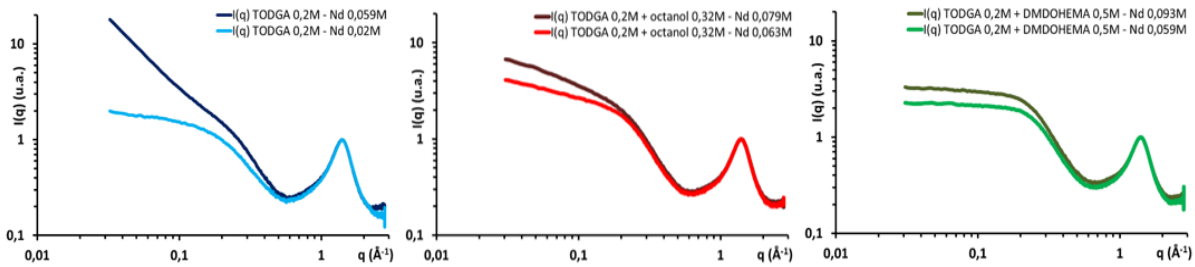

Figure 8. Experimental SWAXS Intensities of the organic phases: TODGA 0.2M (blue), TODGA 0.2M + 5% octanol (red) and TODGA 0.2M + DMDOHEMA 0.5M (green) in heptane after extraction of neodymium nitrate.

Adding 5% octanol results in SWAXS intensities similar for both concentration of neodymium in the organic phase with a slightly higher intensity for the highest $Nd(NO_3)_3$ concentration. The shape of these curves is similar to the shape of the SWAXS curve of the organic phase containing TODGA 0.2M without octanol at low neodymium concentration: it suggests the formation of small species, even at the highest 0.06M neodymium concentration. The absence of a clear plateau and the small but continuous increase of the signal in the small angles area suggests a polydispersity of the aggregates formed at both neodymium concentrations.

For the organic phases with TOGDA 0.2M + DMDOHEMA 0.5M, the SWAXS intensities are different: after a small intensity increase around 0.4 $Å^{-1}$, a plateau is observed in the small angle area. This suggests the formation of small (and finite sized) aggregates similar to those observed in DMDOHEMA organic phases without TODGA.

MOLECULAR DYNAMIC SIMULATION

Molecular dynamic simulations have been performed for the six organic phases containing neodymium nitrate with composition of the solutions issuing from the experimental analysis (as reported in Table 3). Snapshots of the MD simulation boxes as well as the corresponding SWAXS intensity are reported on Figure 9.

This project has received funding from the EURATOM research and training programme 2014–2018 under grant agreement No 730227

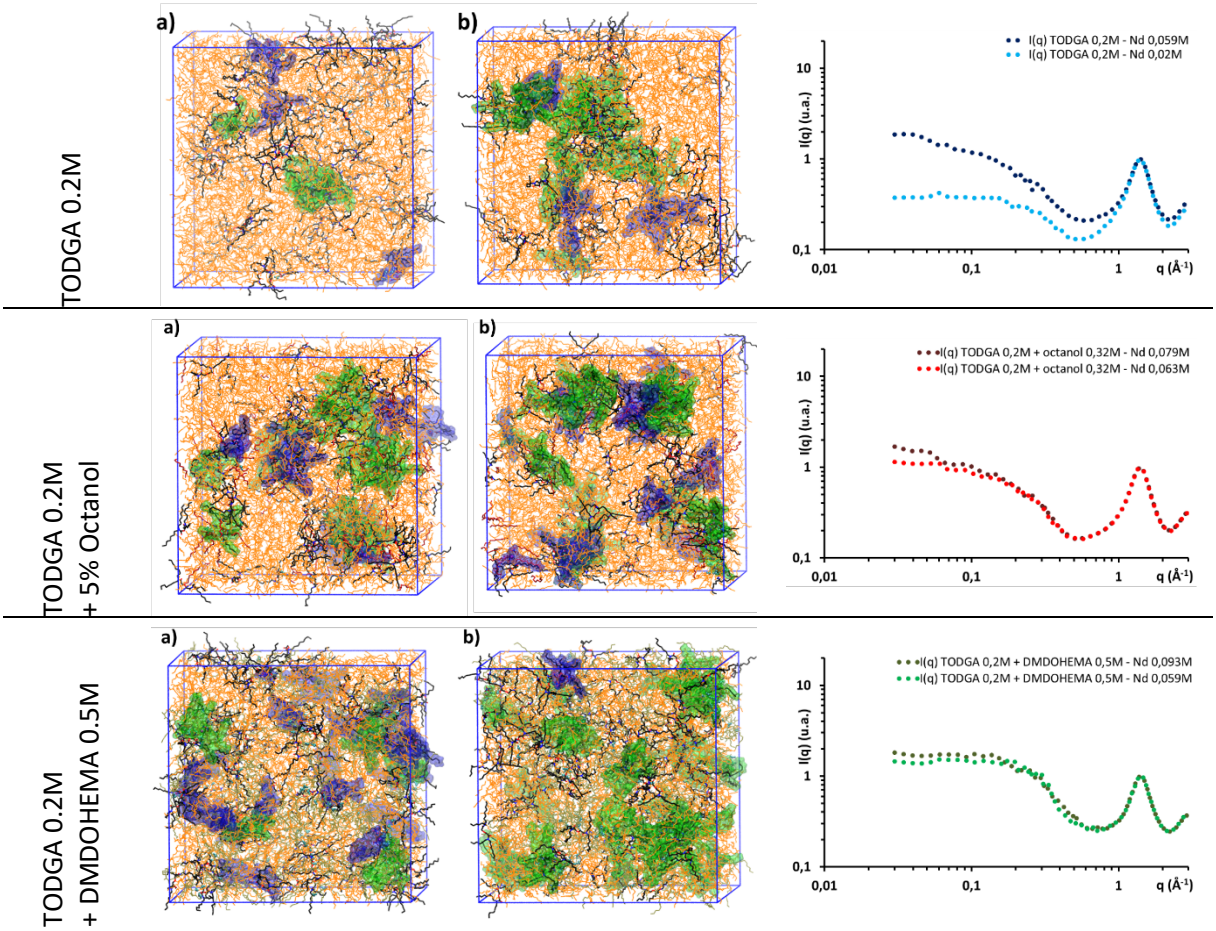

Figure 9. MD boxes simulation snapshots for: a) low and b) high neodymium nitrate concentrations and corresponding calculated SWAXS intensities in TODGA 0.2M (first line), TODGA 0.2M + 5% octanol (second line) and TODGA 0.2M + DMDOHEMA 0.5M (last line) in heptane after extraction of neodymium nitrate. Heptane: orange, carbon atoms: black, nitrogen atoms: blue and oxygen atoms: red. The monometallic complexes or aggregates are highlighted in blue and the polymetallic aggregates are highlighted in green.

TODGA 0.2M IN N-HEPTANE

The molecular dynamics simulations trajectories analysis shows that; when TODGA is used as the extractant, without any phase modifier or co-extractant, mainly polymetallic species are formed. Even at low neodymium concentration in the organic phase ($[Nd]_{org}$ = 0.019M), only 44% neodymium are involved in monometallic complexes. The proportion of monometallic complexes decrease to 14% when the neodymium concentration is increase to 0.059M (i.e. close to the segregation concentration) in the organic phase. In these polymetallic aggregates (mainly bi, tri and tetra-metallic aggregates), the neodymium cations are bonded by bridging nitrates ions (3 per Nd^{3+}) and surrounded by TODGA extractant (2 per Nd^{3+}) and water molecules (1 to 2 per Nd^{3+}).

This project has received funding from the EURATOM research and training programme 2014–2018 under grant agreement No 730227

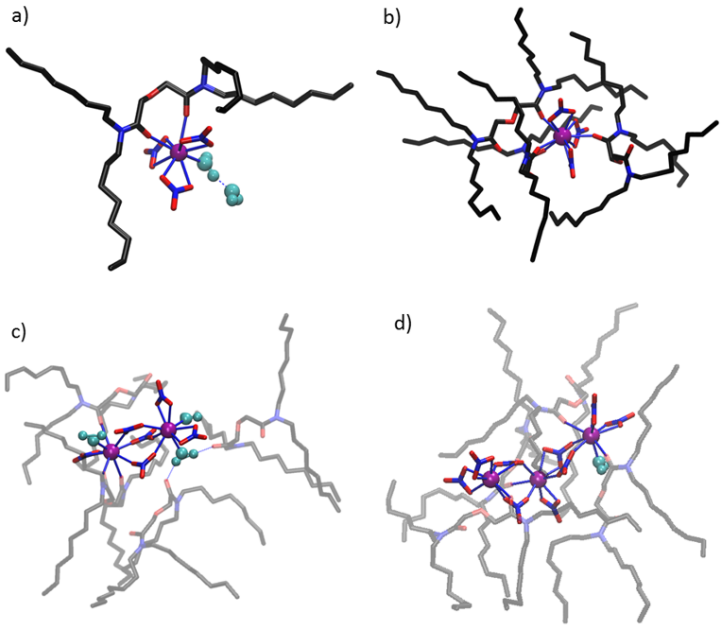

Figure 10. Representative structures observed in the TODGA 0.2M simulations after extraction of neodymium nitrate. Neodymium: purple, carbon atoms in black, nitrogen atoms in blue and oxygen atoms in red. TODGA hydrogen atoms are not represented, water molecules are represented in cyan

TODGA 0.2M + 5% OCTANOL IN N-HEPTANE

For a similar neodymium concentration in the organic phase, the introduction of 0.32M octanol (0.2M TODGA + 5%Vol octanol) decreases the number of polymetallic aggregates: for $[Nd]_{org}$ = 0.063M the proportion of monometallic complexes raises to 34% (14% without octanol). The size of the polymetallic aggregates also decreases: almost no aggregates with more than 3 neodymium are formed. The radial distribution function of the octanol oxygen atoms centred on Nd^{3+} shows that, on the average, each Nd^{3+} is bonded to 1 octanol, decreasing the number of water molecules in the cation first coordination sphere.

Surprisingly, increasing the neodymium concentration in this 0.2M TODGA + 5% octanol organic phase does not lead to an increase of the aggregation: on the contrary, the number of monometallic complexes even increase to 45%, and the number of larger aggregate decreases in favour of the smaller bimetallic aggregates.

Octanol molecules are included in these aggregates, replacing the few water molecules that were bonded to the neodymium cation in the organic phase without octanol. The presence of these octanol molecules stabilizes the aggregates, increases the solubility of the aggregates in the organic phase and avoids their coalescence, preventing the segregation of the organic phase at higher $Nd(NO_3)_3$ concentration. Octanol is therefore not a “simple” phase modifier since it takes part directly in the complexes or aggregates structure and enhances their solubility by addition of aliphatic chains near the extracted cation.

This project has received funding from the EURATOM research and training programme 2014–2018 under grant agreement No 730227

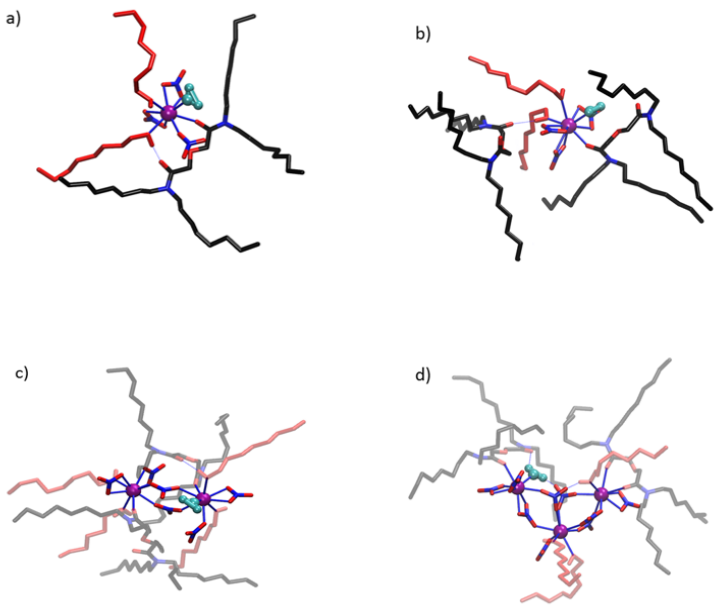

Figure 11. Representative structures observed in the TODGA 0.2M + 5% octanol simulations after extraction of neodymium nitrate. Neodymium: purple, carbon atoms in black, nitrogen atoms in blue and oxygen atoms in red. TODGA hydrogen atoms are not represented; octanol molecules are represented in red, water molecules are represented in cyan.

TODGA 0.2M + DMDOHEMA 0.5M IN N-HEPTANE

The addition of 0.5M DMDOHEMA as an alternative of octanol (0.2M TODGA + 0.5M DMDOHEMA) and for a comparable neodymium concentration (0.06M) decreases drastically the aggregation: in this case, 73% of the $Nd(NO_3)_3$ present in the organic phase are included in monometallic complexes. The DMDOHEMA extractant truly act as a co-extractant: DMDOHEMA molecules are involved in the complexation of the Nd^{3+} cation, replacing TODGA extractants.

The loading capacity of this organic phase is much higher than the two previous ones, and even for $[Nd]_{org}$ = 0.093M, the size of the aggregates remains small (around 80% of the neodymium form mono or bimetallic complexes or aggregates). This aggregate size reduction is concomitant with a reduction of the aggregates polar core size reduction, which consequently reduces the attraction between these polar cores, and therefore the possible coalescence of these aggregates. The DMDOHEMA extractant is here the major one (its concentration is more than twice higher than the TODGA one), therefore, even if TODGA molecules are still present in all the aggregates, the organic phase structure is here imposed by the DMDOHEMA extractant (and not TODGA).

This project has received funding from the EURATOM research and training programme 2014–2018 under grant agreement No 730227

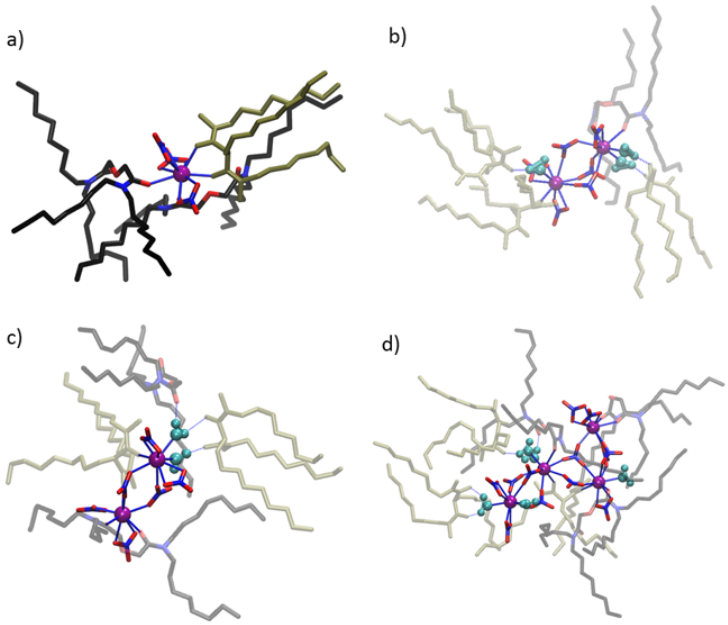

Figure 12. Representative structures observed in the TODGA 0.2M + DMDOHEMA 0.5M simulations after extraction of neodymium nitrate. Neodymium: purple, carbon atoms in black, nitrogen atoms in blue and oxygen atoms in red. TODGA and DMDOHEMA hydrogen atoms are not represented, DMDOHEMA molecules are represented in light brown, water molecules are represented in cyan.

CONCLUSION

The characterization of organic phases containing either TODGA 0.2M, TODGA 0.2M + 5% 1-octanol (corresponding to 0.32M) or TODGA 0.2M + 0.5M DMDOHEMA, in n-heptane has been performed, allowing to better understand the role of phase modifier (n-octanol) or co-extractant (DMDOHEMA) in organic solutions.

Without metallic cation, in 0.2M TODGA solution in n-heptane, small aggregates containing mainly two or three TODGA molecules represent 74 % of the extractants. These results are consistent with literature data. [6, 32-33] The extraction of $Nd(NO_3)_3$ by this organic phase leads to complexes or aggregates where each neodymium is surrounded by water molecules, nitrate ions, and several TODGA extractants with some in the cation second coordination sphere. MD simulation results show that neodymium cations are bonded in average to 2 to 4 TODGA, 3 nitrate ions and 1 to 2 water molecules. Simulations show as well that polymetallic species (aggregates) may be formed in the organic phase, even for low neodymium concentrations. An increase of Nd^{3+} concentration results in an increase of the aggregates sizes that can lead to a third phase formation, in agreement with the experimental results. Adding 5% octanol (0.32M) to 0.2M TODGA solution in n-heptane leads to the formation of mixed aggregates that contain 1 to 3 TODGA and 1 to 4 octanol molecules. These mixed aggregates (which represent 60% of the TODGA molecules) solvate more water than the aggregates formed with TODGA only. In the organic phases containing 0.2M TODGA and 0.5M DMDOHEMA, the DMDOHEMA extractants drive the organization: all the aggregates contain at least one DMDOHEMA molecule. Some aggregates containing only DMDOHEMA are even observed. Each of them solvates water molecules.

This project has received funding from the EURATOM research and training programme 2014–2018 under grant agreement No 730227

After $Nd(NO_3)$ extraction, and for a similar neodymium concentration, the ESI-MS studies in presence of 5% vol. octanol or 0.5M DMDOHEMA show that the number of TODGA around each neodymium decreases. Mixed complexes or aggregates are formed, with at least one TODGA molecule remaining in the cation's first coordination sphere. The MD simulations indicates the formation of complexes and aggregates including both TODGA + octanol (in presence of 5% vol. of octanol) and TODGA + DMDOHEMA (in presence of 0.5M DMDOHEMA). In presence of octanol, some octanol molecules replace water molecules in the cation first coordination spheres. Octanol molecules act as a co-surfactant, improving the solubility of the neodymium species in the organic phase, but with a direct contribution in the aggregate structures. With 0.5M DMDOHEMA in the organic phase, the MD simulations show that DMDOHEMA molecules replace partially TODGA in the cation first coordination sphere. In the aggregates, the phase modifier (octanol) replaces water molecules, whereas the co-extractant replaces the other extractant.

Intrinsically, octanol and DMDOHEMA have much lower interactions with Nd^{3+} than TODGA: alcohol are less polar than amide, and DMDOHEMA extracts much less neodymium than TODGA (at low nitric acid concentration D_{Nd} is around 100 times smaller for an organic phase with [DMDOHEMA] = 0.7M than an organic phase with [TODGA] = 0.1M [1-2, 52]). However, **these results show that at the concentrations used in the *i*-SANEX and EURO-GANEX processes (0.32M octanol or 0.5M DMDOHEMA respectively), these molecules both interact directly with the extracted salts in the organic phase, modifying the structure of the neodymium species, and improving their solubility in this organic phase**. In other words, the TODGA extractant, which remains in the cation first coordination sphere in both cases, preserves its significant role in the complexation/selectivity of the cations, but both octanol and DMDOHEMA have a significant role in the speciation of these cations in the organic phase.

MATERIALS AND METHODS

MATERIALS

TODGA and DMDOHEMA were synthesized by pharmasynthese company (purity by GC-FID > 99%). 1-octanol and n-heptane was used without further purification (Sigma-Aldrich, anhydrous > 99%). The organic phases were prepared by dissolving weighed amounts of reagent.

Aqueous neodymium nitrate solutions were prepared by dissolution of hexahydrated neodymium (III) nitrate obtained from prolabo (purity > 99%) into a solution of 3 mol·L^{-1} lithium nitrate (at reagent grade-Prolabo) 0.01 mol.L^{-1} nitric acid with deionized water produced by the milli-Q Plus apparatus (Millipore).

SOVENT EXTRACTION

WATER EXTRACTION:

Organic solutions were contacted with deionized water with a V_{org}/V_{aq} volume ratio of 1. Extraction were performed at room temperature (25°C) with 30 min stirring. Aqueous and organic phases were separated after 5 minutes centrifugation.

This project has received funding from the EURATOM research and training programme 2014–2018 under grant agreement No 730227

NEODYMIUM NITRATE EXTRACTION:

Extractions were conducted by contacting suitable volumes of an aqueous phase with an organic phase to reach the targeted Nd(III) concentration in the organic phase (see Table 5). Extraction were performed at room temperature (25°C) with 30 min stirring then aqueous and organic phases were separated after centrifugation for 5 minutes. The experimental conditions (V_{org}/V_{aq}, and compositions of the initial aqueous and organic phases are reported in Table 5).

***Table 5*. Composition of the initial aqueous and organic solutions. Vorg/Vaq represent the ratio between organic / aqueous solution's volumes for the neodymium extraction.**

	Initial aqueous phase	***Initial organic phase***	V_{org}/V_{aq}
TODGA 0.2M Nd 0.019M	*$Nd(NO_3)_3$ 0.02M $LiNO_3$ 3M HNO_3 10^{-2}M*	*TODGA 0.2M in n-heptane*	*1/1*
TODGA 0.2M Nd 0.059M	*$Nd(NO_3)_3$ 0.05M $LiNO_3$ 3M HNO_3 10^{-2}M*		*1/1.28*
TODGA 0.2M Octanol 0.32M Nd 0.063M	*$Nd(NO_3)_3$ 0.05M $LiNO_3$ 3M HNO_3 10^{-2}M*	*TODGA 0.2M Octanol 0.32M in n-heptane*	*1/1.28*
TODGA 0.2M Octanol 0.32M Nd 0.079M			*1/2*
TODGA 0.2M DMDOHEMA 0.5M Nd 0.059M	*$Nd(NO_3)_3$ 0.05M $LiNO_3$ 3M HNO_3 10^{-2}M*	*TODGA 0.2M DMDOHEMA 0.5M in n-heptane*	*1/1.28*
TODGA 0.2M DMDOHEMA 0.5M Nd 0.093M			*1/2*

TITRATION

WATER CONCENTRATION:

To determine the equilibrium concentration of water in each organic phase, Karl Fischer titrations were performed on a Metrohm 831KF coulometer with a range of detection between 10 µg and 10 mg of water. The reliability of the method was checked by the measurement of water content in a standard sample (Hydranal – Water standard 1.0 from Riedel de Haëns). The titrations were performed at least in triplicate to provide an estimated uncertainty of less than ± 5 %.

ND CONCENTRATION

Neodymium concentration were determined by ICP-AES. Analyses were performed with a JobinYvon 2000S ICPAES. After extraction in the organic phase, metallic cations were stripped by 0.01 mol.L^{-1} HNO_3 aqueous phase (1/100 organic/aqueous phase volume ratio) and then diluted 0.3M HNO_3 before ICP-AES analysis. Reference solutions of neodymium (III) nitrate in the range 1-50 mg·L^{-1} were used for calibration.

DENSITY MEASUREMENT

Density measurements of the organic solutions were performed at 25°C using an Anton Paar Stabinger viscosimeter SVM 300.

This project has received funding from the EURATOM research and training programme 2014–2018 under grant agreement No 730227

FT-IR SPECTROSCOPY.

Infrared measurements were performed using a Bruker Equinox 55 FTIR spectrometer equipped with an ATR (attenuated total reflectance) cell. All spectra were collected between 650 and 4000 cm^{-1} using 32 scans and a resolution of 2 cm^{-1}.

ESI-MS MASS SPECTROMETRY.

The mass spectrometry measurements were recorded in positive ionization mode using a Bruker Daltonics micrOTOF-Q II quadrupole time-of-flight mass spectrometer equipped with an electrospray interface. A syringe infusion pump, Cole Palmer, delivered the sample at a rate of 180 $\mu L \cdot h^{-1}$ to the electrospray source. The QTOF was mass calibrated daily using an Agilent (G1969-85000) ESI Low concentration tuning solution. The capillary voltage was set to −4500 V with an end-plate offset voltage of −500 V. Nitrogen was employed as the drying and nebulizing gas. The drying gas flow rate was set to 4.0 $L \cdot min^{-1}$, the nebulizing gas pressure was set to 0.4 bar, and the source temperature was set to 180 °C. Spectra were acquired over a mass range of m/z 40–3000. Tandem mass spectra were obtained from collision-induced dissociation (CID) with nitrogen. All samples were diluted by a factor of 1000 to 10000 in an acetonitrile/water (50/50) mixture prior to any injection into the ESI-MS. Species were identified by comparison with an isotopic pattern calculated using the DataAnalysis 4.0 software.

SMALL AND WIDE ANGLE X-RAY SCATTERING

Small and wide-angle X-ray scattering (SWAXS) experiments were carried out on a bench built by Xenocs and using Mo radiation (λ= 0.71 Å). Collimation was applied using a 12:∞ multilayer Xenocs mirror (for Mo radiation) coupled to two sets of Forvis scatterless slits providing a 0.8 mm × 0.8 mm X-ray beam at the sample position. 2mm diameter quartz capillaries containing the samples were used. A large on-line 2D scanner detector (MAR Research 345) located at 750 mm from the sample stage was used to record the scattered beam. A large q-range (2×10^{-1} to 30 nm^{-1}) with q defined as $q = [(4\pi)/\lambda]\sin(\vartheta/2)$ was covered thanks to off-centre detection (ϑ being the scattering angle). Data pre-analysis was performed using FIT2D software to transform isotropic 2D scattering in 1D scattering curves. Absolute intensities in cm^{-1} were obtained using either a 2.36 mm thick high-density polyethylene sample (from Goodfellow®) as a calibration standard or water for which the level of scattering at low q is known ($1.64.10^{-2}$ cm^{-1}).

MOLECULAR DYNAMIC SIMULATIONS

Molecular dynamic (MD) simulations have been performed using the AMBER 14 software with the parm99 force field [53] and taking explicitly into account all atoms polarization effects. Water molecules were described using the POL3 model [54]. The polarizable models for Nd^{3+}, NO_3^- and n-heptane are described in previously published studies [55]. Atomic partial charges on TODGA, DMDOHEMA and 1-octanol were calculated using the restricted electrostatic potential (RESP) procedure [56-57]. The MD simulation boxes compositions were defined based on the corresponding experimental analyses of the organic phases, for which all compounds concentrations have been determined (see Table 5 and Table 3). Initial MD simulation boxes were built using a random distribution of the corresponding molecules. These systems were then equilibrated at 300 K and 1 atm during at last 2ns. After checking the equilibration by assessing the stability of classical parameters such as the volume, density and kinetic energy of the simulated box, production runs were subsequently collected during 5 to 10 ns. The equation of motion was numerically integrated using a 1 fs time step, and simulations were carried out in the NPT ensemble, using a 15 Å truncation cut-off, applying periodic boundary conditions to the simulation boxes and particle mesh Ewald for the long-range interactions calculation. SWAXS intensities were computed taking into account the whole MD trajectories using the nMoldyn software.[58] The trajectories were then analysed computing radial distribution functions in order to determine the aggregation cut-off distances and the corresponding aggregates populations were counted using the CPPTRAJ AmberTools module[59]

This project has received funding from the EURATOM research and training programme 2014–2018 under grant agreement No 730227

Ln(III) AND Pu(IV) LOADING EXPERIMENTS WITH DGA SOLVENTS

KIT: P. Wessling, T. Sittel, P. J. Panak and A. Geist

INTRODUCTION

The extraction of Ln(III) and Pu(IV) into various diglycolamide (DGA) based solvents was studied under loading conditions. Solvents studied were:

- *N,N,N',N'*-tetra-*n*-octyl diglycolamide (TODGA, Figure 13 left) + 5 vol-% 1-octanol in TPH
- TODGA in 1,4-diisopropyl benzene (DIPB)
- 2*R*,2*S'*-oxybis-(*N,N*-didecyl) propanamide (*cis*-mTDDGA, Figure 13 right) in Exxsol D80

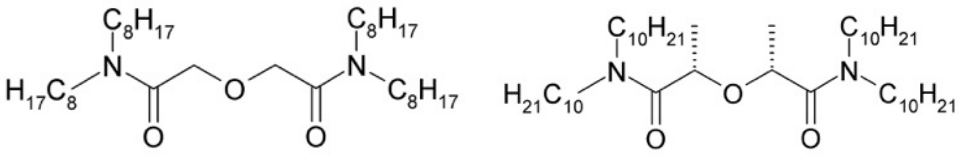

Figure 13. TODGA (left) and *cis*-mTDDGA (right).

TODGA SOLVENTS: Ln(III) LOADING

TODGA + 5% 1-OCTANOL IN TPH: LN(III) LOADING EXPERIMENTS

Various stoichiometries (1:2, 1:3 and 1:4) are reported for the extraction of Ln(III) with diglycolamide extracting agents.[1] Spectroscopic investigations indicate that the major complexes formed in the extraction of An(III) and Ln(III) by TODGA are 1:3 complexes.[60] This is supported by a Nd(III) loading experiment.[3] However, distribution data collected in the SACSESS project cannot be described correctly without the presence of 1:2 complexes, which is also supported by equilibrium modelling performed in GENIORS.

Three loading experiments were performed in support of the equilibrium modelling activities:

- La(III) extraction from 3 mol/L HNO_3
- Nd(III) extraction from 1 mol/L HNO_3 (in contrast to[3] which used 3 mol/L HNO_3)
- Yb(III) extraction from 3 mol/L HNO_3

In any case, the solvent was 0.1 mol/L TODGA + 5% octanol in TPH. The La(III) and Nd(III) experiments were spiked with ^{241}Am(III). ^{214}Am(III) activities in organic and aqueous phases were determined by gamma counting. Due to the rather high metal ion concentrations a gamma absorption correction was applied. Ln(III) concentrations in organic and aqueous phases were determined by ICP-MS; organic phase samples were stripped into a glycolate solution (0.5 mol/L ammonium glycolate, pH = 4).

This project has received funding from the EURATOM research and training programme 2014–2018 under grant agreement No 730227

Additionally, the organic phase HNO_3 concentration was determined in some of the Nd(III) extraction samples.

The La(III) loading experiment (Figure 14) was initially carried out to an initial aqueous La(III) concentration of 0.1 mol/L. The results pointed to the formation of 1:3 complexes. However, when the experiment was extended to higher initial aqueous La(III) concentrations (up to 1 mol/L) it became apparent that full saturation of the organic phase had not been achieved at 0.1 mol/L La(III). The further results indicate the formation of 1:2 complexes for high initial aqueous La(III) concentrations.

A similar behaviour was observed for the Nd(III) loading experiment (Figure 15). Here, too, the formation of 1:2 complexes for high aqueous Nd(III) concentrations must be considered. The experiment was performed at a lower HNO_3 concentration for modelling purposes, *i.e.* to confirm whether the model would describe the smooth transition towards saturation.

To verify equilibrium distribution models, HNO_3 distribution data under loading were determined. The data (Figure 16) show that HNO_3 is initially expelled from the organic phase due to Nd(III) loading; beyond 0.1 mol/L initial aqueous Nd(III) concentration the organic HNO_3 concentration starts increasing. This is explained by the formation of Nd(III) complexes containing additional molecules of HNO_3.

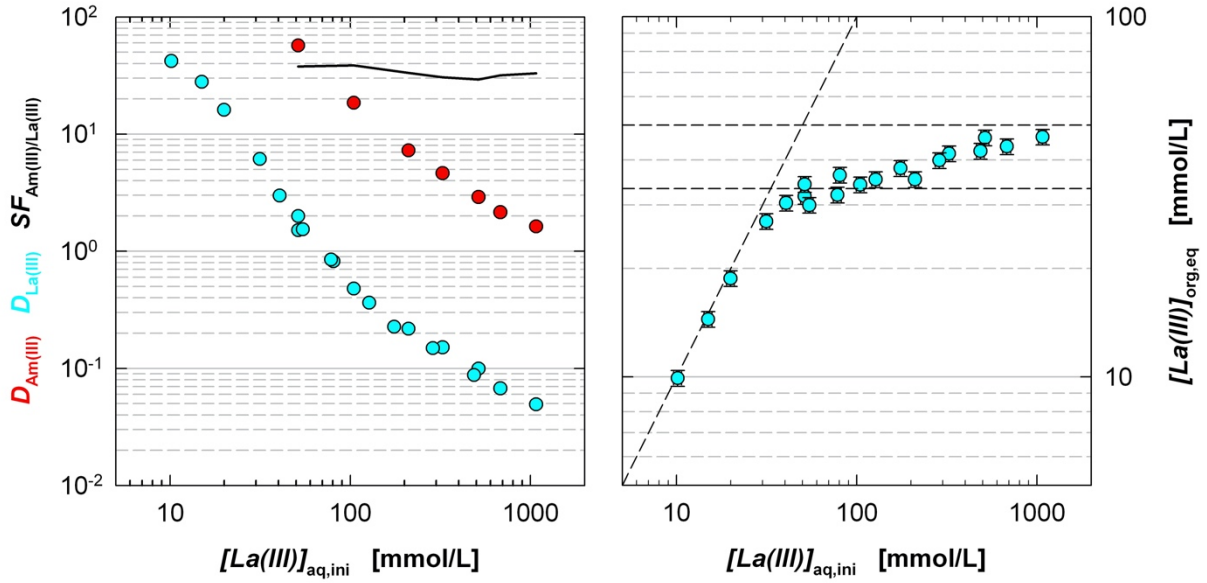

Figure 14. Extraction of La(III) and Am(III) from HNO_3 into TODGA. *Left,* distribution ratios and separation factor as a function of aqueous initial La(III) concentration. *Right,* organic equilibrium La(III) concentration as a function of aqueous initial La(III) concentration. The dashed horizontal lines represent the maximum organic La(III) concentration for the 1:3 complex (lower line) and for the 1:2 complex (upper line). Organic phase, 0.1 mol/L TODGA + 5% octanol in TPH. Aqueous phase, $La(NO_3)_3$ + ^{241}Am(III) in 3 mol/L HNO_3. *T* = 293 K. *O/A* = 1.

This project has received funding from the EURATOM research and training programme 2014–2018 under grant agreement No 730227

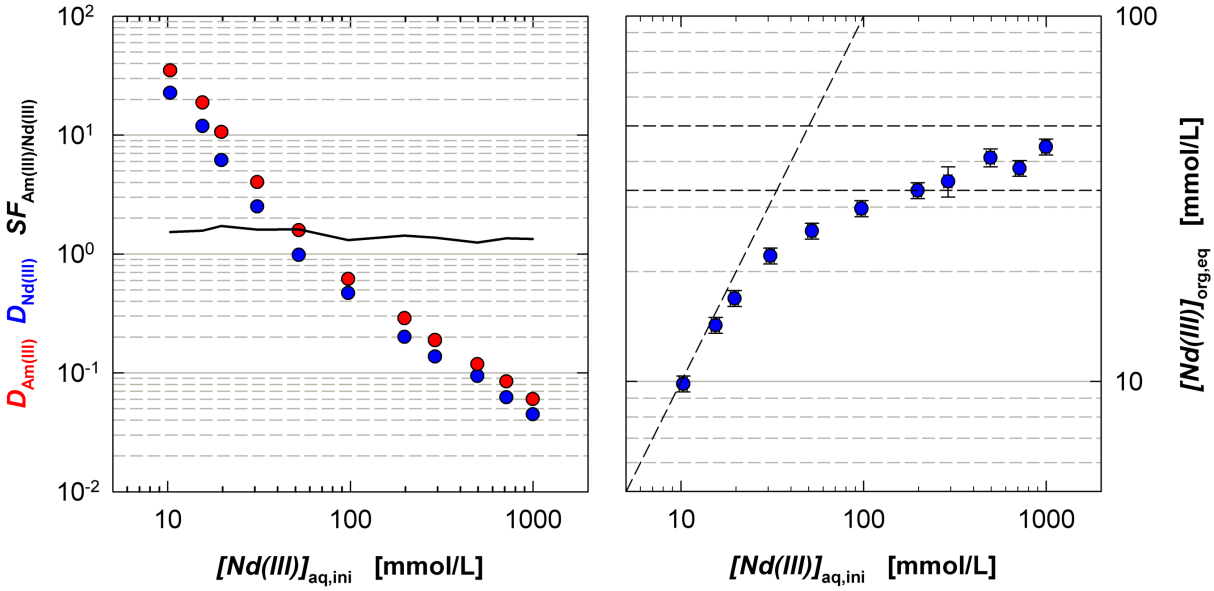

Figure 15. Extraction of Nd(III) and Am(III) from HNO_3 into TODGA. *Left,* distribution ratios and separation factor as function of aqueous initial Nd(III) concentration. *Right,* organic equilibrium Nd(III) concentration as a function of aqueous initial Nd(III) concentration. The dashed horizontal lines represent the maximum organic Nd(III) concentration for the 1:3 complex (lower line) and for the 1:2 complex (upper line). Organic phase, 0.1 mol/L TODGA + 5% octanol in TPH. Aqueous phase, $Nd(NO_3)_3$ + ^{241}Am(III) in 1 mol/L HNO_3. *T* = 293 K. *O/A* = 1.

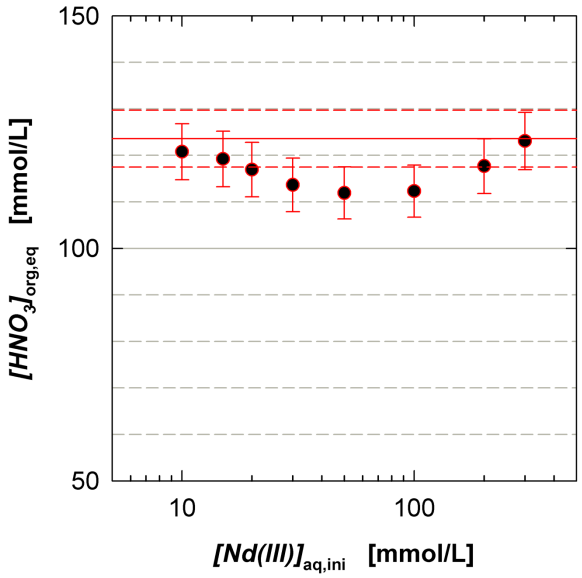

Figure 16. Extraction of Nd(III) and HNO_3 from HNO_3 into TODGA. Organic equilibrium HNO_3 concentration as a function of aqueous initial Nd(III) concentration. Experimental conditions cf. Figure 15. Solid line is $[HNO_3]_{org,eq}$ at $[Nd(III)]_{aq,ini}$ = 0 (dashed lines, ± 5%).

The Yb(III) loading experiment agrees with the formation of a 1:3 complex for the experimental conditions applied, see Figure 17. Since a plateau was observed for 35 mmol/L < $[Yb(III)]_{aq,ini}$ < 90 mmol/L, no further measurements were performed.

This project has received funding from the EURATOM research and training programme 2014–2018 under grant agreement No 730227

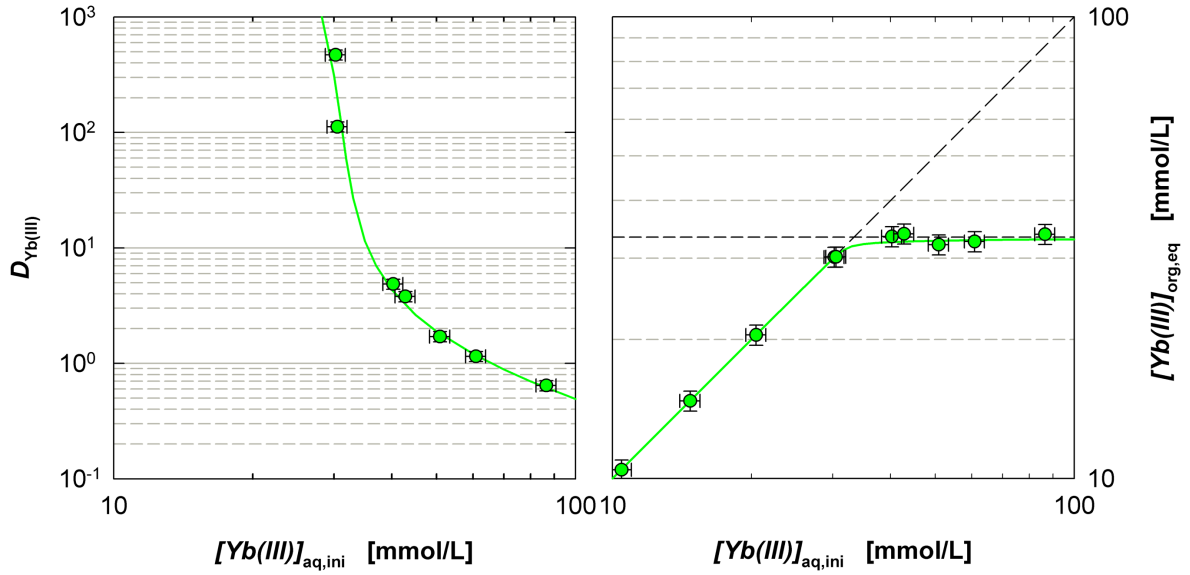

Figure 17. Extraction of Yb(III) from HNO_3 into TODGA. Left, distribution ratios as a function of aqueous initial Yb(III) concentration. Right, organic equilibrium Yb(III) concentration as a function of aqueous initial Yb(III) concentration. The dashed horizontal line represents the maximum organic Yb(III) concentration for the 1:3 complex. Organic phase, 0.1 mol/L TODGA + 5% octanol in TPH. Aqueous phase, $Yb(NO_3)_3$ in 3 mol/L HNO_3. *T* = 293 K. *O/A* = 1. Lines are calculated for the formation of a 1:3 complex.

TODGA IN DIPB: La(III) LOADING EXPERIMENT

Organic diluents such as 1,4-diisopropyl benzene (DIPB) were investigated as an alternative to the octanol/TPH diluent.[61]

To determine the loading capacity of TODGA in DIPB, varying La(III) concentrations (0.01 – 1.84 mol/L) in 1 mol/L HNO_3 were extracted into 0.1 mol/L TODGA in DIPB (Figure 18). No 3rd phase formation was observed. An organic phase La(III) concentration corresponding to the formation of a 1:3 complex was reached at an initial La(III) concentration of 0.45 mol/L. Organic phase La(III) concentrations > 0.033 mol/L were found for initial La(III) concentrations > 0.5 mol/L, indicating the formation of a 1:2 complex.

This project has received funding from the EURATOM research and training programme 2014–2018 under grant agreement No 730227

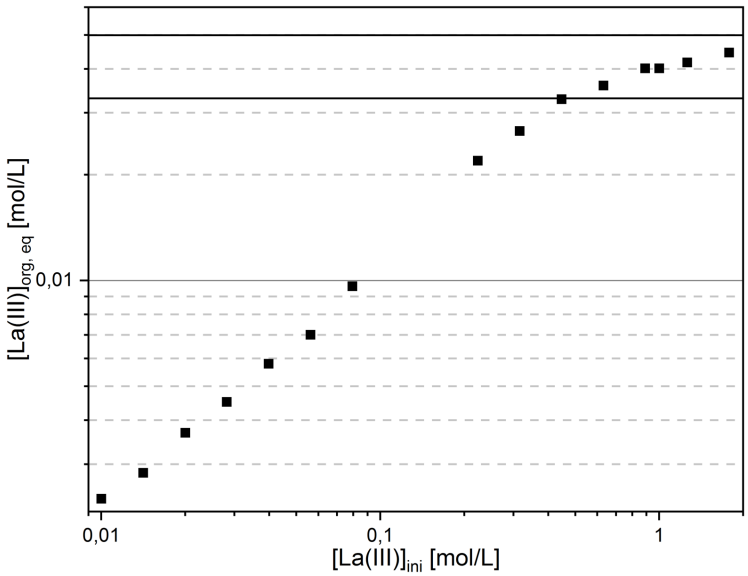

Figure 18. La(III) loading isotherm for the extraction of La(III) with TODGA dissolved in DIPB. Organic phase, 0.1 mol/L TODGA in DIPB. Aqueous phase, $La(NO_3)_3$ in 1 mol/L HNO_3. *T* = 293 K. *O/A* = 1.

TODGA LOADED WITH Ln(III): SPECTROSCOPIC INVESTIGATIONS

To support the existence of the 1:2 complex, TRLFS was performed on loaded organic phases.[61] Aqueous phases containing 1.84 mol/L of M(III) (M = La, Nd, Sm, Gd, Eu) and 10^{-5} mol/L Eu(III) (in case of Sm(III): 10^{-4} mol/L Eu(III)) were contacted with organic phases (0.1 mol/L TODGA in DIPB). After extraction and phase separation the loaded organic phases were investigated by TRLFS, focusing on the Eu(III) emission bands.

Figure 19 shows the normalised Eu(III) fluorescence spectra of the $^5D_0 \rightarrow {}^7F_n$ (left: n = 1, 2; right: n = 0) transitions. Due to the different spectroscopic properties of each lanthanide, only qualitative comparisons between the different systems are possible. In case of Nd(III) and Sm(III), no $^7F_0$ emission bands were detected. Also, in case of Sm(III), a delay of 470 µs was required to detect the Eu(III) fluorescence signal.

In case of organic phases loaded with La(III) and Nd(III) an emission spectrum with emission bands at 592.8 nm, 614.1 nm and 618.8 nm was observed (Figure 19, left). This spectrum corresponds to the $[Eu(TODGA)_3]^{3+}$ complex.[60] However, with the organic phases loaded with Sm(III), Eu(III) or Gd(III) an emission band at 617.9 nm appeared, being most pronounced in the samples containing Gd(III) and Eu(III). This emission band corresponds to neither $[Eu(TODGA)]^{3+}$ (emission band at 615 nm) nor $[Eu(TODGA)_3]^{3+}$ (cf. La(III) and Nd(III) sample). Presumably the observed spectra belong to the $[Eu(TODGA)_2]^{3+}$ complex (which has never been observed in prior studies).

This project has received funding from the EURATOM research and training programme 2014–2018 under grant agreement No 730227

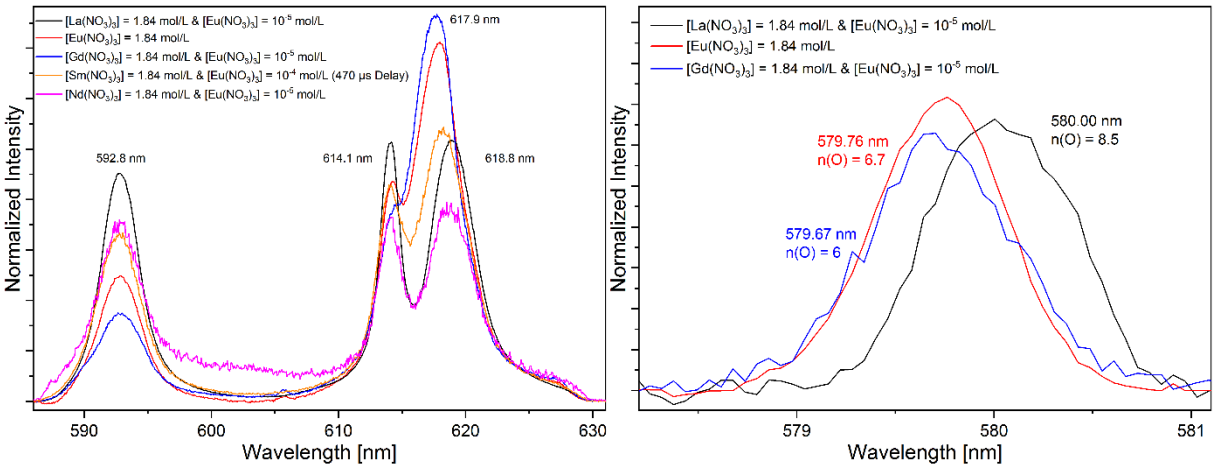

Figure 19. Normalised Eu(III) fluorescence emission spectra of the $^5D_0 \rightarrow {}^7F_n$ transitions (left: *n* = 1, 2; right: *n* = 0) of TODGA solvent samples loaded with Ln(III) (La, Nd, Sm, Eu, Gd). Organic phase, 0.1 mol/L TODGA in DIPB. Aqueous phase, 1.84 mol/L $Ln(NO_3)_3$ in 1 mol/L HNO_3. *T* = 293 K. *O/A* = 1.

Eu(III) emission spectra of the $^5D_0 \rightarrow {}^7F_0$ transition are shown in Figure 19 (right). The shift of the emission band with respect to the emission band of the solvent spectrum (578.9 nm) allows calculating the number of coordinating oxygen donors.[62] In case of La(III) the emission band is found at 580 nm. The calculated number of oxygen donors is 8.5, in good agreement with the $[Eu(TODGA)_3]^{3+}$ complex. In case of Gd(III) and Eu(III), emission bands at 579.67 nm and 579.87 nm are detected, corresponding to 6 and 6.7 oxygen donors, indicating the presence of a 1:2 complex in the loaded organic phase.

Eu(III) fluorescence lifetimes are reported in Table 6. The corresponding lifetime measurements are shown in Figure 20. In case of the La(III) loaded solvent, the lifetime of the Eu(III) emission corresponds to the $[Eu(TODGA)_3]^{3+}$ complex. In case of the Eu(III) loaded solvent, the lifetime of the Eu(III) emission corresponds to the $[Eu(TODGA)_2]^{3+}$ complex. In case of Nd(III), the Eu fluorescence is quenched by Nd(III). In case of Gd(III) and Sm(III), lifetimes corresponding to both $[Eu(TODGA)_3]^{3+}$ and $[Eu(TODGA)_2]^{3+}$ complexes are found.

Table 6. Fluorescence lifetimes of the different loaded organic phases for the extraction with TODGA dissolved in DIPB.

M(III)	Lifetime
La-Eu	1929 µs, $n(H_2O) = -0.1$
Eu	1585 µs, $n(H_2O) = 0.1$
Gd-Eu	short = 926 µs, $n(H_2O) = 0.5$; long = 1929 µs; $n(H_2O) = 0.1$
Sm-Eu	Sm = 44 µs; short = 1094 µs; $n(H_2O) = 0.3$; long = 3424 µs; $n(H_2O) = -0.3$
Nd-Eu	Nd = 1.5 µs; 265 µs; $n(H_2O) = 3.4$

This project has received funding from the EURATOM research and training programme 2014–2018 under grant agreement No 730227

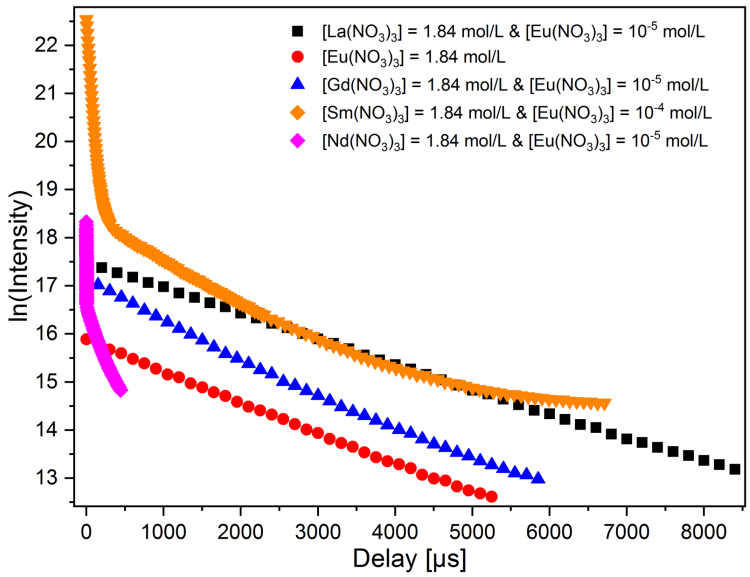

Figure 20. Decrease of the logarithmic intensity as a function of the delay time.

Finally, similar loading experiments were conducted using 0.1 mol/L TODGA dissolved in TPH + 5 vol.% 1-octanol. The Eu(III) spectra in TPH (dashed lines) are shown in Figure 21 (left) and compared to the spectra in DIPB (continuous lines). No significant differences are observed for any of the samples: the presence of a 1:2 complex is evident in Eu(III) and Gd(III) loaded organic phases. This is also supported by the fluorescence lifetime measurements in which the fluorescence lifetime of the Eu(III) and Gd(III) samples is shorter by almost 1600 µs compared to the La(III) sample, Figure 21 (right).

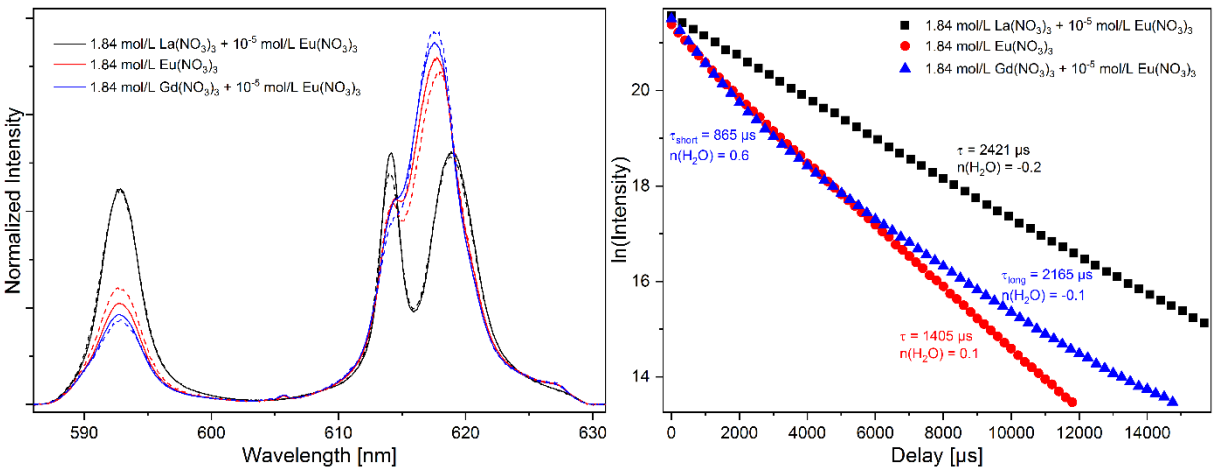

Figure 21. Left, comparison of the normalised Eu(III) fluorescence emission spectra of the $^5D_0 \rightarrow {}^7F_n$ transitions (n = 1,2) of the loaded organic phases of extraction experiments with TODGA dissolved in DIPB (continuous lines) and TPH + 5 vol.% 1-octanol (dashed lines). Right, decrease of the logarithmic fluorescence intensity in TPH + 5 vol.% 1-octanol as a function of the delay time. Organic phases, 0.1 mol/L TODGA in DIPB or TPH + 5 vol.% 1-octanol, loaded by contacting with aqueous phases containing 1.84 mol/L $M(NO_3)_3$ (M = La, Eu, Gd) in 1 mol/L HNO_3. T = 293 K. O/A = 1.

These results are the first spectroscopic evidence of a Eu(III)-TODGA 1:2 complex that is found in Sm(III), Eu(III) or Gd(III) loaded organic phases, independent of the diluent. A trend is observed for the

This project has received funding from the EURATOM research and training programme 2014–2018 under grant agreement No 730227

formation of this complex; it is only found if the distribution ratio of the excess lanthanide is equal to or greater than the distribution ratio of Eu(III). In case of La(III) loaded solvents, Eu(III) is able to displace La(III) and thus forms the $[Eu(TODGA)_3]^{3+}$ complex.

Fluorescence lifetime measurements and $^7F_0$ shifts state that the new species is a 1:2 complex, which explains the observed high lanthanide concentrations in the organic phase of loading experiments and slopes < 3 found in extraction experiments.

TODGA Ln(III) LOADING: CONCLUSIONS

Combining results from slope analysis and spectroscopic investigations of TODGA solvents loaded with Ln(III) with earlier spectroscopic results performed under non-loading conditions[60] leads to the following conclusion:

TODGA extracts Ln(III) (and also An(III)[60]) as 1:3 complexes, $[M(TODGA)_3]^{3+}$ under non-loading conditions (i. e. [M(III)] < 3 × [TODGA]). However, loading in excess of the concentrations viable with the formation of a 1:3 complex is observed for very high initial aqueous M(III) concentrations, which is explained by the formation of a 1:2 complex under these conditions. Consequently, the formation of a 1:2 TODGA complex must be accounted for in equilibrium models.

Pu(IV) LOADING EXPERIMENTS

In support of the development of an improved EURO-GANEX process, Pu(IV) loading studies of two DGA based solvents were performed: a solvent comprising 0.5 mol/L TODGA in DIPB[61] and a solvent comprising 0.5 mol/L *cis*-mTDDGA in Exxsol D80.[63]

PREPARATION OF A Pu(IV) STOCK SOLUTION

Intended for these loading studies, a Pu(IV) stock solution with a Pu(IV) concentration of ≥ 50 g/L was prepared.

1.5 g PuO_2 was dissolved in concentrated HNO_3 and refluxed for 10 h, resulting in complete dissolution. The volume of the solution was reduced to 5 mL. 13 mL of 1 mol/L HNO_3 were added to set the acid concentration to approximately 5 mol/L. UV/Vis spectroscopy in 5 mol/L HNO_3 showed that the solution was ≈ 75 % Pu(IV) and ≈ 25% Pu(VI) (Figure 22 left, black line). Pu(VI) was reduced to Pu(IV) by addition of H_2O_2. The solution was then heated to 70°C to destroy excess H_2O_2.

UV-Vis spectroscopy revealed pure Pu(IV) (Figure 22 left, green line). The solution was analysed by ICP-MS, alpha and gamma spectroscopy, LSC and acid-base titration.

The final solution is 68 g/L (0.28 mol/L) Pu(IV)-239 in 5.9 mol/L HNO_3 (Figure 22 right). It furthermore contains 0.1 g/L U-235, 0.6 g/L Pu-240, 1.5 mg/L Pu-241 and 9 mg/L Am-241.

This project has received funding from the EURATOM research and training programme 2014–2018 under grant agreement No 730227

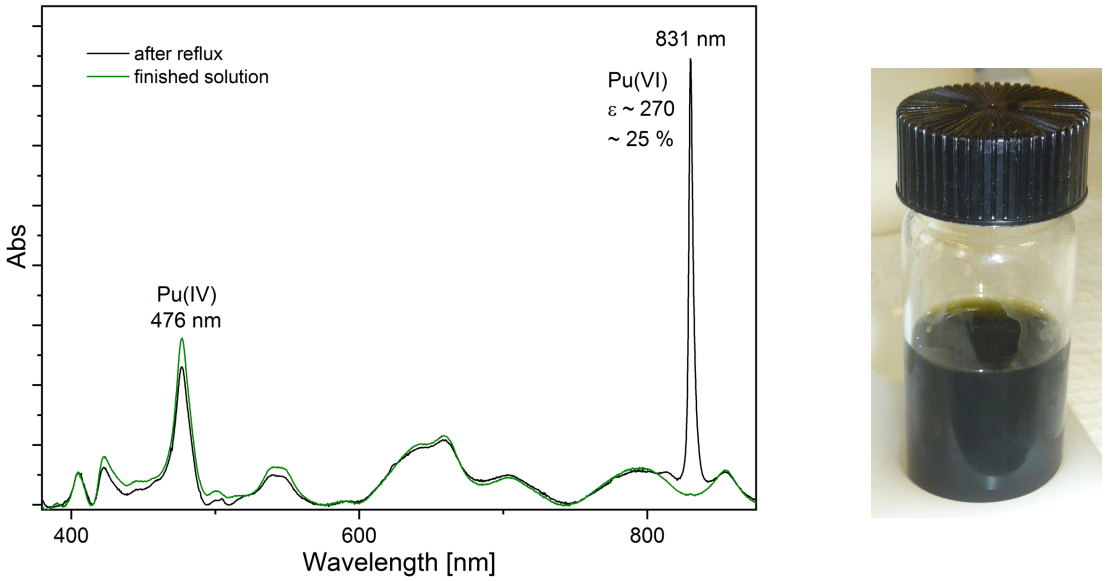

Figure 22. Left, absorption spectra of the Pu dissolution solution after dissolution (black line) and after reduction with H_2O_2 (green line). Right, final Pu(IV) stock solution: 68 g/L Pu(IV) in 5.9 mol/L HNO_3.

TODGA IN DIPB: Pu(IV) LOADING EXPERIMENT

The Pu(IV) loading capacity of the TODGA-DIPB solvent was tested contacting solutions containing 0.5–40 g/L (2.1–170 mmol/L) Pu(IV) in 5 mol/L HNO_3 with equal volumes of 0.5 mol/L TODGA in DIPB at 22 °C.

The loading limit is between 8.3 g/L and 12 g/L initial aqueous Pu(IV) concentration, see Figure 23. The 12 g/L sample contains a precipitate at the phase boundary. The precipitate in the 40 g/L sample is slant due to centrifugation, pointing out its high viscosity.

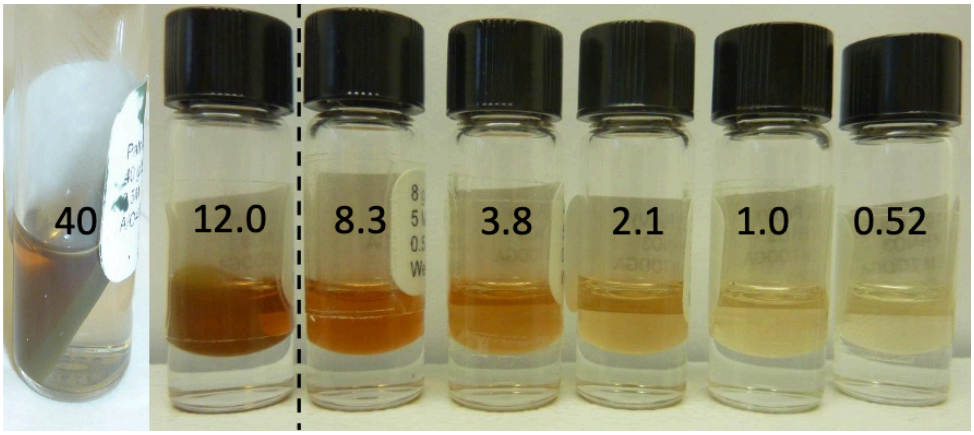

Figure 23. TODGA-DIPB solvent, Pu(IV) loading tests. Organic phase, 0.5 mol/L TODGA in DIPB. Aqueous phase, 0.5–40 g/L (2.1–170 mmol/L) Pu(IV) in 5 mol/L HNO_3. *O/A* = 1, *T* = 22 °C. Numerals indicate initial Pu(IV) concentration [g/L] in aqueous phase, dashed vertical line indicates third phase boundary. Note that the brownish colour of the organic phases is caused by the artificial light in the fume hood.

This project has received funding from the EURATOM research and training programme 2014–2018 under grant agreement No 730227

Organic phase Pu(IV) concentrations in the 0.52–8.3 g/L samples were determined by ICP-MS. This was done in two ways, (a) from the difference between initial and equilibrium aqueous phase concentrations and (b) after stripping the organic phase twice using a solution of 4 mol/L acetohydoxamic acid (AHA) in 0.3 mol/L HNO_3 *(O/A* = 0.1).

Pu(IV) distribution ratios from the first stripping step using AHA are shown in Figure 24. The distribution ratios are in the range of 0.067–0.28. With the phase ratio of *O/A* = 0.1, this corresponds to a stripping efficiency of 99.3% – 97.3%. Consequently, stripping twice is almost quantitative.

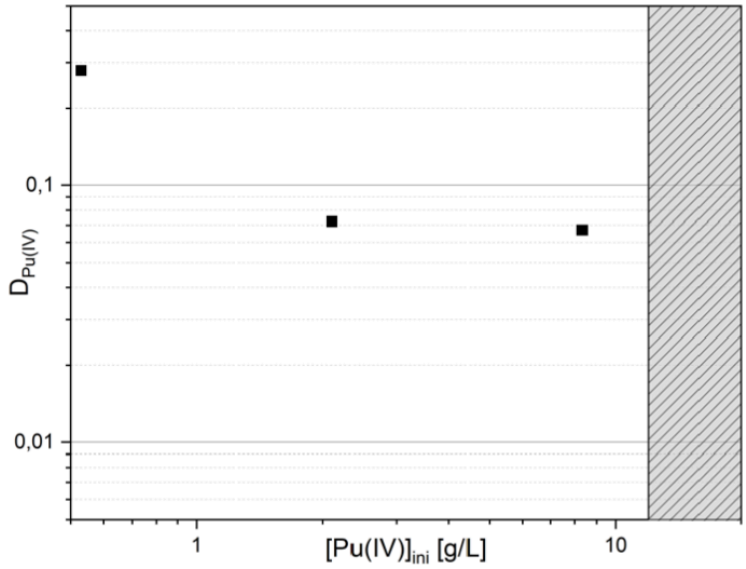

Figure 24. Pu(IV) distribution ratios from the first AHA stripping step. Organic phase, 0.5 mol/L TODGA in DIPB loaded with Pu(IV) from 5 mol/L HNO_3. Aqueous phase, 4 mol/L AHA in 0.3 mol/L HNO_3. *O/A* = 0.1, *T* = 22 °C.

The Pu(IV) loading isotherm is shown in (Figure 25 top), Pu distribution ratios are shown in Figure 25 bottom. The organic phase Pu(IV) concentrations determined by methods (a) and (b) are in good agreement. A slight decrease in Pu(IV) ratios observed with increasing loading might be due to a saturation effect. However, it needs to be considered that the uncertainties of distribution ratios in the range of 10^5 may be considerably higher than the uncertainties of lower distribution ratios (which typically are in the range of 10–20%).

This project has received funding from the EURATOM research and training programme 2014–2018 under grant agreement No 730227

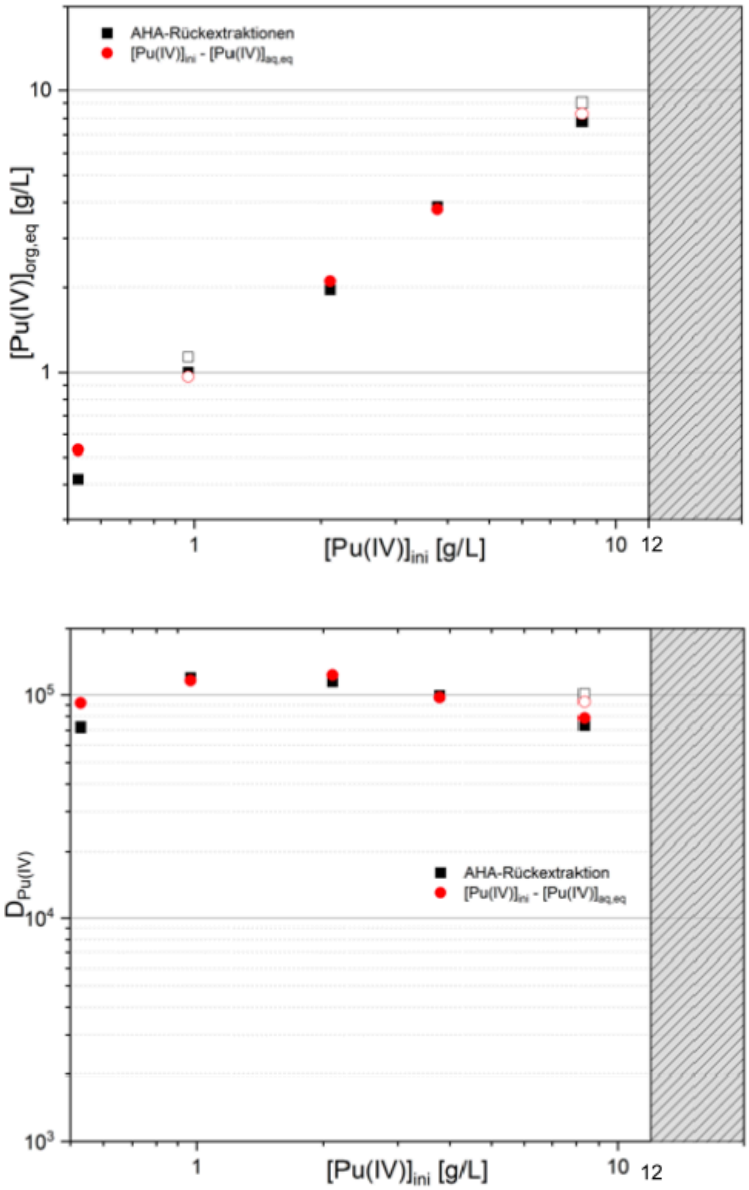

Figure 25. TODGA-DIPB solvent, Pu(IV) loading tests. Top, Pu(IV) loading isotherm. Bottom, Pu(IV) distribution ratios. Organic phase, 0.5 mol/L TODGA in DIPB. Aqueous phase, 0.5–40 g/L (2.1–170 mmol/L) Pu(IV) in 5 mol/L HNO_3. *O/A* = 1, *T* = 22 °C. Organic phase Pu(IV) concentrations determined by stripping with AHA (black symbols) or from aqueous phase mass balance (red symbols).

TODGA IN DIPB: CONCLUSION

With a Pu(IV) loading capacity of < 12/g/L (50 mmol/L) at 5 mol/L HNO_3, the solvent 0.5 mol/L TODGA in DIPB is not suitable for GANEX 2nd cycle applications.

cis-MTDDGA IN EXXSOL D80: Pu(IV) LOADING EXPERIMENTS

cis-mTDDGA was synthesised as described in the literature.[64] The *cis: trans* ratio was 98:2, see the ^{1}H NMR signals at 4.2 ppm and 4.4 ppm (Figure 26).

This project has received funding from the EURATOM research and training programme 2014–2018 under grant agreement No 730227

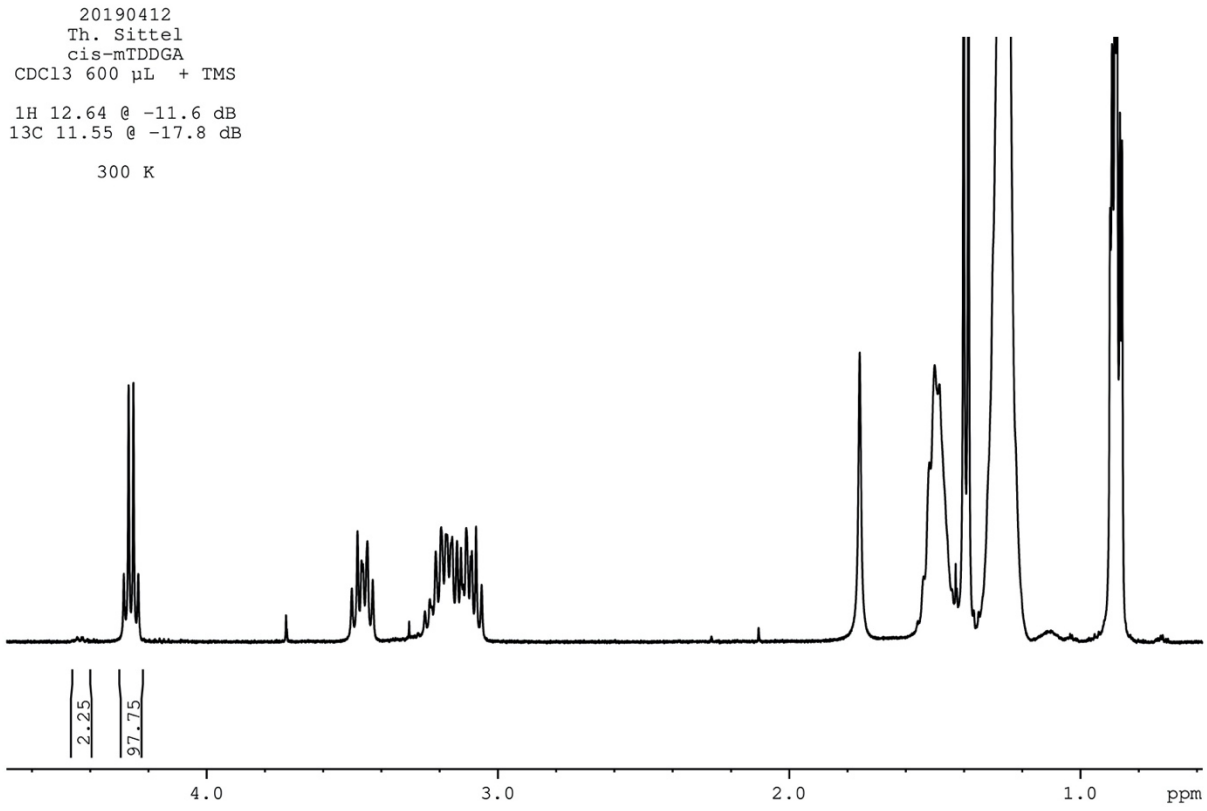

Figure 26. *cis*-mTDDGA, ^{1}H NMR spectrum ($CDCl_3$).

The Pu(IV) loading capacity of the *cis*-mTDDGA solvent was tested contacting solutions containing 2.1–48 g/L (8.8–200 mmol/L) Pu(IV) in 5 mol/L HNO_3 with equal volumes of 0.5 mol/L *cis*-mTDDGA in Exxsol D80 at 22 °C.

Results are shown in Figure 27. Although not directly evident due to the intense colour of the organic phases at elevated Pu(IV) concentrations, none of the samples contained a third phase or a precipitate. These findings do not agree with earlier results for *cis*-mTDDGA,[63] stating the formation of a precipitate at an initial Pu(IV) concentration of 48 g/L in 5 mol/L HNO_3. However, the diluent used was *n*-dodecane rather than Exxsol D80. This demonstrates the advantage of using a kerosene (i. e. branched alkane) diluent, as also observed in other studies, see e. g. reference.[4]

This project has received funding from the EURATOM research and training programme 2014–2018 under grant agreement No 730227

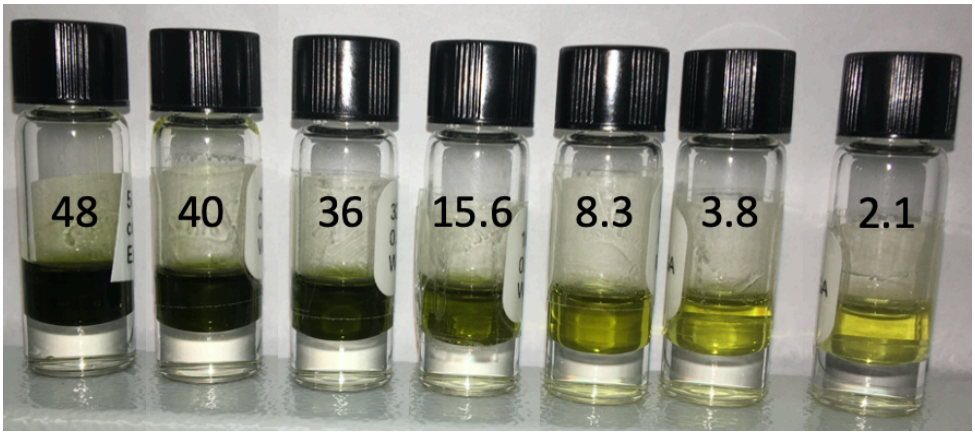

Figure 27. *cis*-mTDDGA solvent, Pu(IV) loading tests. Organic phase, 0.5 mol/L *cis*-mTDDGA in Exxsol D80. Aqueous phase, 2.1–48 g/L (8.8–200 mmol/L) Pu(IV) in 5 mol/L HNO_3. *O/A* = 1, *T* = 22 °C. Numerals indicate initial Pu(IV) concentration [g/L] in aqueous phase.

Organic phase Pu(IV) concentrations were determined as described for the TODGA-DIPB solvent. Results are shown in Figure 28. With distribution ratios in the range of 0.052–0.17 and *O/A* = 0.1, Pu(IV) was stripped to 99.5% – 98.3% already in the first step.

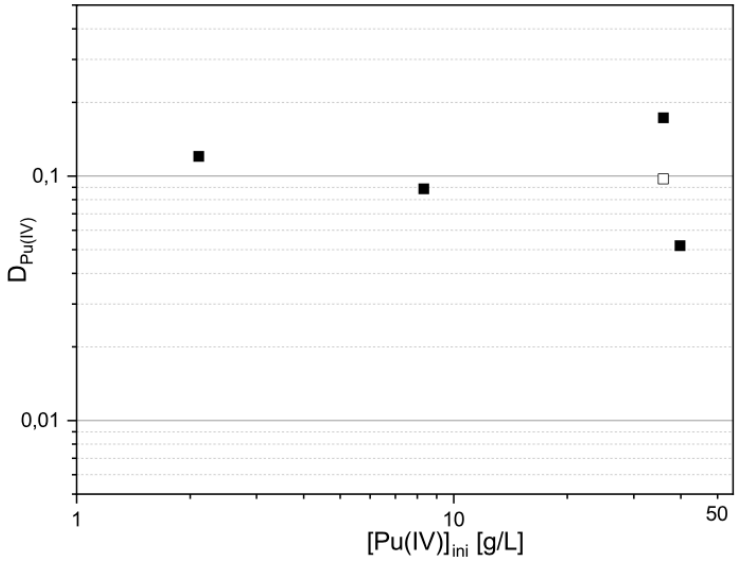

Figure 28. Pu(IV) distribution ratios from the first AHA stripping step. Organic phase, 0.5 mol/L *cis*-mTDDGA in Exxsol D80 loaded with Pu(IV) from 5 mol/L HNO_3. Aqueous phase, 4 mol/L AHA in 0.3 mol/L HNO_3. *O/A* = 0.1, *T* = 22 °C.

The loading isotherm and the distribution ratios for the extraction of Pu(IV) into *cis*-mTDDGA are shown in Figure 29. The organic phase Pu(IV) concentrations determined by methods (a) and (b) are in good agreement.

This project has received funding from the EURATOM research and training programme 2014–2018 under grant agreement No 730227

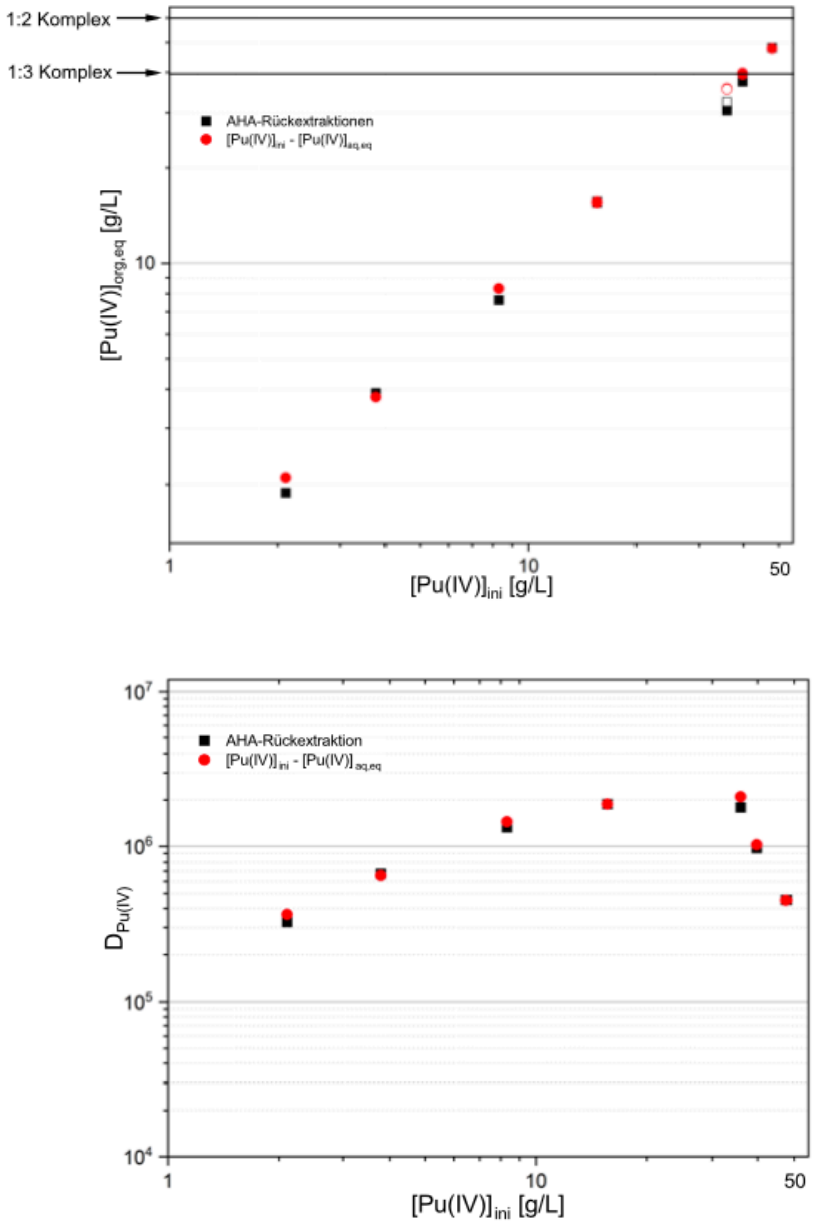

Figure 29. *cis*-mTDDGA solvent, Pu(IV) loading tests. Top, Pu(IV) loading isotherm. Bottom, Pu(IV) distribution ratios. Organic phase, 0.5 mol/L TODGA in DIPB. Aqueous phase, 2.1–48 g/L (8.8–200 mmol/L) Pu(IV) in 5 mol/L HNO_3. *O/A* = 1, *T* = 22 °C. Organic phase Pu(IV) concentrations determined by stripping with AHA (black symbols) or from aqueous phase mass balance (red symbols). The horizontal lines in top figure indicate maximum organic Pu(IV) concentration assuming 1:2 and 1:3 complexes, respectively.

An organic phase Pu(IV) concentration of 40 g/L (0.17 mol/L) corresponds to full loading assuming the formation of a 1:3 complex. Consequently, the extraction of 48 g/L (0.20 mol/L) involves formation of a 1:2 complex. Such a behaviour has also been observed in Ln(III) loading experiments with TODGA.[61]

Pu(IV) distribution ratios increase with increasing initial Pu(IV) concentration up to 36 g/L, followed by a sharp decrease. This may be due to opposing effects of increasing nitrate concentration and saturation. It must be considered that distribution ratios in the range of 10^6 are not easily and precisely determined.

This project has received funding from the EURATOM research and training programme 2014–2018 under grant agreement No 730227

CIS-MTDDGA: CONCLUSION

With a Pu(IV) loading capacity of ≥ 48 g/L (0.2 mol/L) at 5 mol/L HNO_3, a solvent comprising 0.5 mol/L *cis*-mTDDGA in Exxsol D80 is superior to the loading behaviour of the original EURO-GANEX solvent (0.2 mol/L TODGA + 0.5 mol/L DMDOHEMA in TPH), for which a limiting initial aqueous phase Pu(IV) concentration of 30 g/L at 4.5 mol/L HNO_3 is reported.[16]

Pu OXIDATION STATE IN TODGA-DIPD AND *cis*-mTDDGA SOLVENTS

The extraction of Pu(IV) into TODGA-DIPB and *cis*-mTDDGA solvents was studied by UV-Vis spectroscopy. Organic phase samples (TODGA in DIPB or mTDDGA in Exxsol D80) were appropriately diluted with solvent and absorption spectra were recorded (Varian Cary 5G, 1 cm cuvettes, unloaded solvent or 5 mol/L HNO_3 in reference cuvette).

Absorption spectra of Pu-loaded TODGA-DIPB (8.3 g/L Pu, dilution = 100; Figure 30 top) and *cis*-mTDDGA-Exxsol D80 (40 g/L Pu, dilution = 200; Figure 30 bottom) solvents are compared to the spectrum of the Pu(IV) stock solution (diluted to 0.68 g/L Pu(IV) in 1 mol/L HNO_3, red lines in Figure 30).

The absorption spectrum of Pu in TODGA-DIPB (Figure 30 top) shows all the features of Pu(IV). Most features are slightly red shifted, as to be expected due to ligand field splitting upon strong complexation. The results indicate that the oxidation state of Pu(IV) is retained in the organic phase.

In contrast, the absorption spectrum of Pu in *cis*-m-TDDGA-Exxsol D80 (Figure 30 bottom) shows significant differences compared to the Pu(IV) spectrum. As evident from the absence of the strong Pu(VI) absorption (expected at approximately 830 nm), these differences point to the presence of Pu(III) in the *cis*-m-TDDGA-Exxsol D80 solvent.

This project has received funding from the EURATOM research and training programme 2014–2018 under grant agreement No 730227

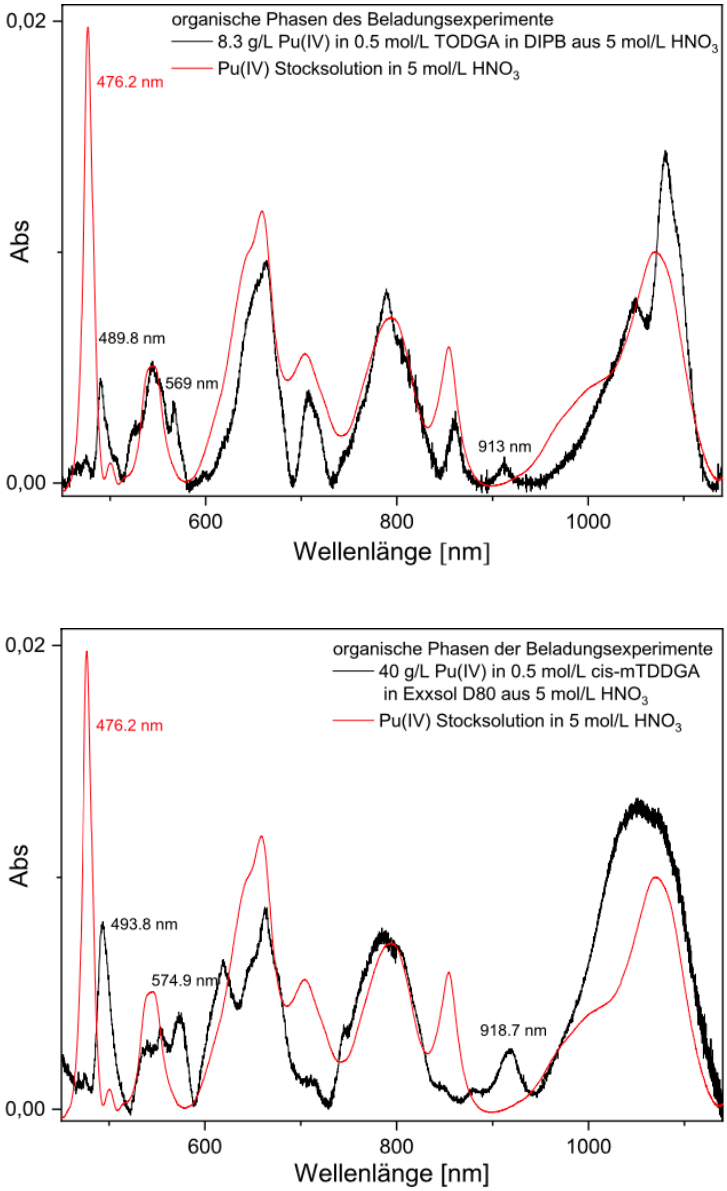

Figure 30. Comparison of Pu absorption spectra in organic phases (black lines) with a spectrum of 0.68 g/L Pu(IV) in 1 mol/L HNO_3 (red lines). Top, 0.083 g/L Pu in the TODGA-DIPB solvent. Bottom, 0.2 g/L Pu in the *cis*-mTDDGA-Exxsol D80 solvent.

To proof the presence of Pu(III) in the *cis*-m-TDDGA-Exxsol D80 solvent, an organic phase Pu(III) reference spectrum was recorded. Pu(III) (prepared by reducing Pu(IV) with hydroxylamine) was extracted into the TODGA-DIPB solvent. The absorption spectrum was recorded in the aqueous phase before extraction (Figure 31 black line) and in the TODGA-DIPB solvent after extraction (Figure 31 red line).

This project has received funding from the EURATOM research and training programme 2014–2018 under grant agreement No 730227

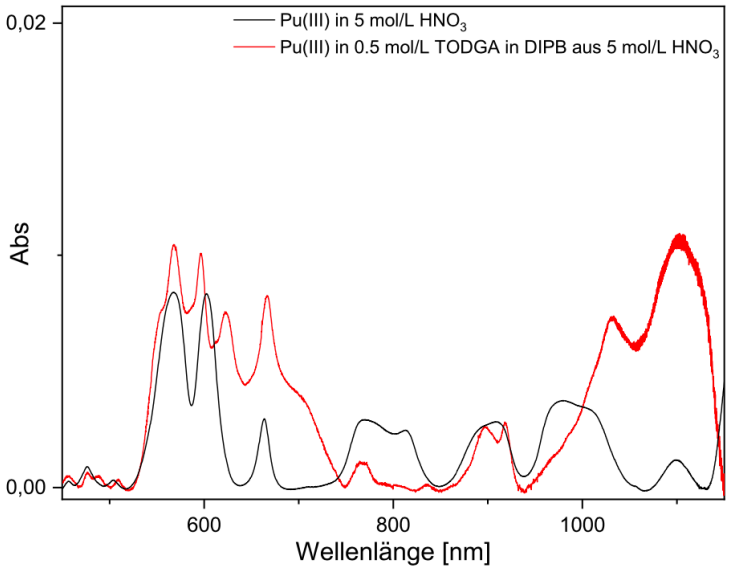

Figure 31. Pu(III) absorption spectra. 0.68 g/L Pu(III) in 1 mol/L HNO_3 (black line) and after extraction into 0.5 mol/L TODGA in DIPB.

Pu(III) in the TODGA-DIPB solvent retains most of the Pu(III) absorption bands. However, the characteristic Pu(III) double band (568.8 nm and 602.4 nm) is triply split (568.8 nm, 596.6 nm, 622.4 nm). The broad band (750–820 nm) loses its intensity.

The Pu absorption spectrum in the *cis*-m-TDDGA-Exxsol D80 solvent is compared to the Pu(III) spectrum in the TODGA-DIPB solvent and the Pu(IV) spectrum in 1 mol/L HNO_3 (Figure 32). The presence of Pu(III) in the *cis*-m-TDDGA-Exxsol D80 solvent is supported by the absorption bands at 574.9 nm, 618.5 nm and 918.7 nm.

These results show a partial reduction of Pu(IV) to Pu(III) upon extraction into a solvent comprising 0.5 mol/L *cis*-m-TDDGA in Exxsol D80.

This project has received funding from the EURATOM research and training programme 2014–2018 under grant agreement No 730227

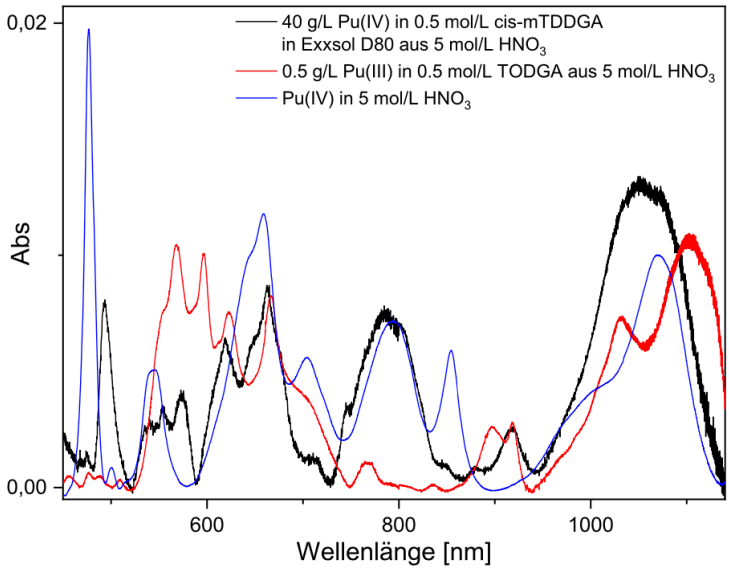

Figure 32. Comparison of the Pu absorption spectrum in the cis-mTDDGA -Exxsol D80 solvent (black line) to the Pu(IV) absorption spectrum in 1 mol/L HNO_3 (blue line) and the Pu(III) absorption spectrum in the TODGA-DIPB solvent (red line).

Pu(IV) LOADING EXPERIMENTS: CONCLUSIONS

A solvent comprising 0.5 mol/L TODGA in DIPB is not useful for EURO-GANEX applications. In contrast, 0.5 mol/L *cis*-mTDDGA in Exxsol D80 is able to extract no less than 48 g/L (0.2 mol/L) Pu(IV) from 5 mol/L HNO_3, making it a promising candidate for further EURO-GANEX process development. As already outlined in the literature,[63] this solvent is also expected to perform better than the TODGA + DMDOHEMA solvent[17-18] with respect to fission product handling.

This project has received funding from the EURATOM research and training programme 2014–2018 under grant agreement No 730227

REFERENCES

1. Ansari, S. A.; Pathak, P.; Mohapatra, P. K.; Manchanda, V. K., Chemistry of diglycolamides: promising extractants for actinide partitioning. *Chem. Rev.* **2012,** *112* (3), 1751–1772.

2. Tachimori, S.; Sasaki, Y.; Suzuki, S.-I., Modification of TODGA-*n*-dodecane solvent with a monoamide for high loading of lanthanides(III) and actinides(III). *Solvent Extr. Ion Exch.* **2002,** *20* (6), 687–699.

3. Geist, A.; Modolo, G., TODGA process development: an improved solvent formulation. In *Proc. Internat. Conf. GLOBAL 2009 (The Nuclear Fuel Cycle: Sustainable Options & Industrial Perspectives)*, Paris, 6–11 September, 2009; pp 1022–1026.

4. Modolo, G.; Asp, H.; Schreinemachers, C.; Vijgen, H., Development of a TODGA based process for partitioning of actinides from a PUREX raffinate part I: batch extraction optimization studies and stability tests. *Solvent Extr. Ion Exch.* **2007,** *25* (6), 703–721.

5. Sasaki, Y.; Sugo, Y.; Suzuki, S.; Kimura, T., A method for the determination of extraction capacity and its application to N,N,N',N'-tetraalkylderivatives of diglycolamide-monoamide/n-dodecane media. *Analytica Chimica Acta* **2005,** *543* (1–2), 31–37.

6. Nave, S.; Modolo, G.; Madic, C.; Testard, F., Aggregation properties of *N,N,N',N'*-tetraoctyl-3-oxapentanediamide (TODGA) in *n*-dodecane. *Solvent Extr. Ion Exch.* **2004,** *22* (4), 527–551.

7. Sasaki, Y.; Zhu, Z.-X.; Sugo, Y.; Suzuki, H.; Kimura, T., Extraction capacity of diglycolamide derivatives for Ca(II), Nd(III) and Zr(IV) from nitric acid to *n*-dodecane containing a solvent modifier. *Analytical Sciences* **2005,** *21* (10), 1171–1175.

8. Whittaker, D.; Geist, A.; Modolo, G.; Taylor, R.; Sarsfield, M.; Wilden, A., Applications of diglycolamide based solvent extraction processes in spent nuclear fuel reprocessing, part 1: TODGA. *Solvent Extr. Ion Exch.* **2018,** *36* (3), 223–256.

9. Geist, A.; Müllich, U.; Magnusson, D.; Kaden, P.; Modolo, G.; Wilden, A.; Zevaco, T., Actinide(III)/lanthanide(III) separation via selective aqueous complexation of actinides(III) using a hydrophilic 2,6-bis(1,2,4-triazin-3-yl)-pyridine in nitric acid. *Solvent Extr. Ion Exch.* **2012,** *30* (5), 433–444.

10. Wilden, A.; Modolo, G.; Kaufholz, P.; Sadowski, F.; Lange, S.; Sypula, M.; Magnusson, D.; Müllich, U.; Geist, A.; Bosbach, D., Laboratory-scale counter-current centrifugal contactor demonstration of an innovative-SANEX process using a water soluble BTP. *Solvent Extr. Ion Exch.* **2015,** *33* (2), 91–108.

11. Modolo, G.; Wilden, A.; Kaufholz, P.; Bosbach, D.; Geist, A., Development and demonstration of innovative partitioning processes (i-SANEX and 1-cycle SANEX) for actinide partitioning. *Progr. Nucl. Energy* **2014,** *72*, 107–114.

12. McLachlan, F.; Taylor, R.; Whittaker, D.; Woodhead, D.; Geist, A., Modelling of innovative SANEX process maloperations. *Proc. Chem.* **2016,** *21*, 109–116.

13. Muller, J. M.; Berthon, C.; Couston, L.; Zorz, N.; Simonin, J.-P.; Berthon, L., Extraction of lanthanides(III) by a mixture of a malonamide and a dialkyl phosphoric acid. *Solvent Extr. Ion Exch.* **2016,** *34* (2), 141–160.

14. Bell, K.; Carpentier, C.; Carrott, M.; Geist, A.; Gregson, C.; Hérès, X.; Magnusson, D.; Malmbeck, R.; McLachlan, F.; Modolo, G.; Müllich, U.; Sypula, M.; Taylor, R.; Wilden, A., Progress towards the development of a new GANEX process. *Proc. Chem.* **2012,** *7*, 392–397.

15. Carrott, M. J.; Gregson, C. R.; Taylor, R. J., Neptunium extraction and stability in the GANEX solvent: 0.2 M TODGA/0.5 M DMDOHEMA/kerosene. *Solvent Extr. Ion Exch.* **2013,** *31* (5), 463–482.

This project has received funding from the EURATOM research and training programme 2014–2018 under grant agreement No 730227

16. Brown, J.; McLachlan, F.; Sarsfield, M.; Taylor, R.; Modolo, G.; Wilden, A., Plutonium loading of prospective grouped actinide extraction (GANEX) solvent systems based on diglycolamide extractants. *Solvent Extr. Ion Exch.* **2012,** *30* (2), 127–141.

17. Carrott, M.; Geist, A.; Hérès, X.; Lange, S.; Malmbeck, R.; Miguirditchian, M.; Modolo, G.; Wilden, A.; Taylor, R., Distribution of plutonium, americium and interfering fission products between nitric acid and a mixed organic phase of TODGA and DMDOHEMA in kerosene, and implications for the design of the "EURO-GANEX" process. *Hydrometallurgy* **2015,** *152*, 139–148.

18. Malmbeck, R.; Magnusson, D.; Bourg, S.; Carrott, M.; Geist, A.; Hérès, X.; Miguirditchian, M.; Modolo, G.; Müllich, U.; Sorel, C.; Taylor, R.; Wilden, A., Homogenous recycling of transuranium elements from irradiated fast reactor fuel by the EURO-GANEX solvent extraction process. *Radiochim. Acta* **2019,** *107* (9–11), 917–929.

19. Pathak, P. N.; Ansari, S. A.; Kumar, S.; Tomar, B. S.; Manchanda, V. K., Dynamic light scattering study on the aggregation behaviour of *N,N,N′,N′*-tetraoctyl diglycolamide (TODGA) and its correlation with the extraction behaviour of metal ions. *J. Colloid Interf. Sci.* **2010,** *342* (1), 114–118.

20. Sasaki, Y.; Rapold, P.; Arisaka, M.; Hirata, M.; Kimura, T.; Hill, C.; Cote, G., An additional insight into the correlation between the distribution ratios and the aqueous acidity of the TODGA system. *Solvent Extr. Ion Exch.* **2007,** *25* (2), 187–204.

21. Ansari, S. A.; Pathak, P. N.; Husain, M.; Prasad, A. K.; Parmar, V. S.; Manchanda, V. K., Extraction of actinides using *N,N,N′,N′*-tetraoctyl diglycolamide (TODGA): a thermodynamic study. *Radiochim. Acta* **2006,** *94* (6–7), 307–312.

22. Suzuki, H.; Sasaki, Y.; Sugo, Y.; Apichaibukol, A.; Kimura, T., Extraction and separation of Am(III) and Sr(II) by *N,N,N′,N′*-tetraoctyl-3-oxapentanediamide (TODGA). *Radiochim. Acta* **2004,** *92* (8), 463–466.

23. Mowafy, E. A.; Aly, H. F., Synthesis of some *N,N,N′,N′*-tetraalkyl-3-oxa-pentane-1,5-diamide and their applications in solvent extraction. *Solvent Extr. Ion Exch.* **2007,** *25* (2), 205–224.

24. Wang, Z.; Huang, H.; Ding, S.; Hu, X.; Zhang, L.; Liu, Y.; Song, L.; Chen, Z.; Li, S., Extraction of trivalent americium and europium with TODGA homologs from HNO_3 solution. *J. Radioanal. Nucl. Chem.* **2017,** *313* (2), 309–318.

25. Sengupta, A.; Ali, S. M.; Shenoy, K. T., Understanding the complexation of the Eu^{3+} ion with TODGA, CMPO, TOPO and DMDBTDMA: Extraction, luminescence and theoretical investigation. *Polyhedron* **2016,** *117*, 612–622.

26. Brigham, D. M.; Ivanov, A. S.; Moyer, B. A.; Delmau, L. H.; Bryantsev, V. S.; Ellis, R. J., Trefoil-shaped outer-sphere ion clusters mediate lanthanide(III) ion transport with diglycolamide ligands. *J. Amer. Chem. Soc.* **2017,** *139* (48), 17350–17358.

27. Baldwin, A. G.; Ivanov, A. S.; Williams, N. J.; Ellis, R. J.; Moyer, B. A.; Bryantsev, V. S.; Shafer, J. C., Outer-sphere water clusters tune the lanthanide selectivity of diglycolamides. *ACS Central Science* **2018,** *4* (6), 739–747.

28. Pathak, P. N.; Ansari, S. A.; Godbole, S. V.; Dhobale, A. R.; Manchanda, V. K., Interaction of Eu^{3+} with *N,N,N′,N′*-tetraoctyl diglycolamide: a time resolved luminescence spectroscopy study. *Spectrochimica Acta Part A: Molecular and Biomolecular Spectroscopy* **2009,** *73* (2), 348–352.

29. Arisaka, M.; Kimura, T., Thermodynamic and spectroscopic studies on Am(III) and Eu(III) in the extraction system of *N,N,N′,N′*-tetraoctyl-3-oxapentane-1,5-diamide in *n*-dodecane/nitric acid. *Solvent Extr. Ion Exch.* **2011,** *29* (1), 72–85.

This project has received funding from the EURATOM research and training programme 2014–2018 under grant agreement No 730227

30. Ellis, R. J.; Brigham, D. M.; Delmau, L.; Ivanov, A. S.; Williams, N. J.; Vo, M. N.; Reinhart, B.; Moyer, B. A.; Bryantsev, V. S., "Straining" to separate the rare earths: how the lanthanide contraction impacts chelation by diglycolamide ligands. *Inorg. Chem.* **2017,** *56* (3), 1152–1160.

31. Testard, F.; Zemb, T.; Bauduin, P.; Berthon, L., Third-phase formation in liquid/liquid extraction: a colloidal approach. *Ion Exchange and Solvent Extraction A Series of Advances* **2010,** *19*, 381-428.

32. Yaita, T.; Herlinger, A. W.; Thiyagarajan, P.; Jensen, M. P., Influence of extractant aggregation on the extraction of trivalent *f*-element cations by a tetraalkyldiglycolamide. *Solvent Extr. Ion Exch.* **2004,** *22* (4), 553–571.

33. Jensen, M. P.; Yaita, T.; Chiarizia, R., Reverse-micelle formation in the partitioning of trivalent *f*-element cations by biphasic systems containing a tetraalkyldiglycolamide. *Langmuir* **2007,** *23* (9), 4765–4774.

34. Ganguly, R.; Sharma, J. N.; Choudhury, N., TODGA based w/o microemulsion in dodecane: an insight into the micellar aggregation characteristics by dynamic light scattering and viscometry. *J. Colloid Interf. Sci.* **2011,** *355* (2), 458–463.

35. Prathibha, T.; Venkatesan, K. A.; Antony, M. P., Comparison in the aggregation behaviour of amide extractant systems by dynamic light scattering and ATR-FTIR spectroscopy. *Colloids and Surfaces A: Physicochemical and Engineering Aspects* **2018,** *538*, 651–660.

36. Singh, M. B.; Patil, S. R.; Lohi, A. A.; Gaikar, V. G., Insight into nitric acid extraction and aggregation of N, N, N', N'-Tetraoctyl diglycolamide (TODGA) in organic solutions by molecular dynamics simulation. *Separ. Sci. Technol.* **2018,** *53* (9), 1361–1371.

37. Suneesh, A. S.; Venkatesan, K. A.; Antony, M. P.; Vasudeva Rao, P. R., Molecular dynamic simulations in diglycolamides-Eu$(NO_3)_3$ system. *Journal of Computational Chemistry and Molecular Modelling* **2016,** *1* (1), 13–19.

38. Guilbaud, P.; Berthon, L.; Louisfrema, W.; Diat, O.; Zorz, N., Determination of the structures of uranyl–tri-*n*-butyl-phosphate aggregates by coupling experimental results with molecular dynamic simulations. *Chem. Eur. J.* **2017,** *23* (65), 16660–16670.

39. Paquet, A.; Diat, O.; Berthon, L.; Guilbaud, P., Aggregation in organic phases after solvent extraction of uranyl nitrate: X-ray scattering and molecular dynamic simulations. *Journal of Molecular Liquids* **2019,** *277*, 22–35.

40. Ferru, G.; Gomes Rodrigues, D.; Berthon, L.; Diat, O.; Bauduin, P.; Guilbaud, P., Elucidation of the structure of organic solutions in solvent extraction by combining molecular dynamics and X-ray scattering. *Angew. Chem. Int. Ed.* **2014,** *53* (21), 5346–5350.

41. Rodrigues, F.; Ferru, G.; Berthon, L.; Boubals, N.; Guilbaud, P.; Sorel, C.; Diat, O.; Bauduin, P.; Simonin, J. P.; Morel, J. P.; Morel-Desrosiers, N.; Charbonnel, M. C., New insights into the extraction of uranium(VI) by an *N,N*-dialkylamide. *Molecular Physics* **2014,** *112* (9–10), 1362–1374.

42. Meridiano, Y.; Berthon, L.; Crozes, X.; Sorel, C.; Dannus, P.; Antonio, M. R.; Chiarizia, R.; Zemb, T., Aggregation in organic solutions of malonamides: consequences for water extraction. *Solvent Extr. Ion Exch.* **2009,** *27* (5–6), 607–637.

43. Ceraulo, L.; Giorgi, G.; Liveri, V.; Bongiorno, D.; Indelicato, S.; Di Gaudio, F.; Indelicato, S., Mass spectrometry of surfactant aggregates. *European Journal of Mass Spectrometry* **2011,** *17*, 525–541

44. Ellis, R. J.; Meridiano, Y.; Muller, J.; Berthon, L.; Guilbaud, P.; Zorz, N.; Antonio, M. R.; Demars, T.; Zemb, T., Complexation-induced supramolecular assembly drives metal-ion extraction. *Chem. Eur. J.* **2014,** *20* (40), 12796–12807.

This project has received funding from the EURATOM research and training programme 2014–2018 under grant agreement No 730227

45. Antonio, M. R.; Chiarizia, R.; Gannaz, B.; Berthon, L.; Zorz, N.; Hill, C.; Cote, G., Aggregation in solvent extraction systems containing a malonamide, a dialkylphosphoric acid and their mixtures. *Separ. Sci. Technol.* **2008,** *43* (9–10), 2572–2605.

46. Berthon, L.; Zorz, N.; Gannaz, B.; Lagrave, S.; Retegan, T.; Fermvik, A.; Ekberg, C., Use of electrospray ionization mass spectrometry for the characterization of actinide complexes in solution. *IOP Conference Series: Materials Science and Engineering* **2010,** *9*, 012059.

47. Rey, J.; Dourdain, S.; Dufrêche, J. F.; Berthon, L.; Muller, J. M.; Pellet-Rostaing, S.; Zemb, T., Thermodynamic description of synergy in solvent extraction: I. Enthalpy of mixing at the origin of synergistic aggregation. *Langmuir* **2016,** *32* (49), 13095–13105.

48. Pecheur, O.; Dourdain, S.; Guillaumont, D.; Rey, J.; Guilbaud, P.; Berthon, L.; Charbonnel, M. C.; Pellet-Rostaing, S.; Testard, F., Synergism in a HDEHP/TOPO liquid-liquid extraction system: an intrinsic ligands property? *J. Phys. Chem. B* **2016,** *120* (10), 2814–2823.

49. Choppin, G. R.; Henrie, D. E.; Buijs, K., Environmental effects on *f-f* transitions. I. Neodymium(III). *Inorg. Chem.* **1966,** *5* (10), 1743–1748.

50. Stephens, E. M.; Schoene, K.; Richardson, F. S., Hypersensitivity in the 4*f*—4*f* absorption spectra of neodymium(III) complexes in aqueous solution. *Inorg. Chem.* **1984,** *23* (12), 1641–1648.

51. Jensen, M. P.; Chiarizia, R.; Urban, V., Investigation of the aggregation of the neodymium complexes of dialkylphosphoric, -oxothiophosphinic, and -dithiophosphinic acids in toluene. *Solvent Extr. Ion Exch.* **2001,** *19* (5), 865–884.

52. Meridiano, Y. *Organisation des molécules extractantes de type diamide : lien avec les propriétés extractantes ?*; Thèse de l'Université Paris-XI. CEA-R- 6228, Commissariat à l'énergie atomique: France, 2009.

53. Case, D. A.; Cheatham, T. E.; Darden, T.; Gohlke, H.; Luo, R.; Merz, K. M.; Onufriev, A.; Simmerling, C.; Wang, B.; Woods, R. J., The Amber biomolecular simulation programs. *Journal of Computational Chemistry* **2005,** *26* (16), 1668-1688.

54. Meng, E. C.; Kollman, P. A., Molecular Dynamics Studies of the Properties of Water around Simple Organic Solutes. *J. Phys. Chem.* **1996,** *100* (27), 11460-11470.

55. Duvail, M.; Ruas, A.; Venault, L.; Moisy, P.; Guilbaud, P., Molecular Dynamics Studies of Concentrated Binary Aqueous Solutions of Lanthanide Salts: Structures and Exchange Dynamics. *Inorganic Chemistry* **2010,** *49* (2), 519-530.

56. Fox, T.; Kollman, P. A., Application of the RESP methodology in the parametrization of organic solvents. *Journal of Physical Chemistry B* **1998,** *102* (41), 8070-8079.

57. Cornell, W. D.; Cieplak, P.; Bayly, C. I.; Gould, I. R.; Merz, K. M.; Ferguson, D. M.; Spellmeyer, D. C.; Fox, T.; Caldwell, J. W.; Kollman, P. a., A 2Nd Generation Force-Field for the Simulation of Proteins, Nucleic-Acids, and Organic-Molecules. *Journal of the American Chemical Society* **1995,** *117* (19), 5179-5197.

58. Rog, T.; Murzyn, K.; Hinsen, K.; Kneller, G. R., nMoldyn: A program package for a neutron scattering oriented analysis of Molecular Dynamics simulations. *Journal of Computational Chemistry* **2003,** *24* (5), 657-667.

59. Roe, D. R.; Cheatham, T. E., PTRAJ and CPPTRAJ: Software for Processing and Analysis of Molecular Dynamics Trajectory Data. *Journal of Chemical Theory and Computation* **2013,** *9* (7), 3084-3095.

60. Wilden, A.; Modolo, G.; Lange, S.; Sadowski, F.; Beele, B. B.; Skerencak-Frech, A.; Panak, P. J.; Iqbal, M.; Verboom, W.; Geist, A.; Bosbach, D., Modified diglycolamides for the An(III) + Ln(III) co-separation: evaluation by

This project has received funding from the EURATOM research and training programme 2014–2018 under grant agreement No 730227

solvent extraction and time-resolved laser fluorescence spectroscopy. *Solvent Extr. Ion Exch.* **2014,** *32* (2), 119–137.

61. Weßling, P.; Müllich, U.; Guerinoni, E.; Geist, A.; Panak, P. J., Solvent extraction of An(III) and Ln(III) using TODGA in aromatic diluents to suppress third phase formation. *Hydrometallurgy* **2020,** *192*, 105248.

62. Choppin, G. R.; Wang, Z. M., Correlation between ligand coordination number and the shift of the $^7F_0$–$^5D_0$ transition frequency in europium(III) complexes. *Inorg. Chem.* **1997,** *36* (2), 249–252.

63. Malmbeck, R.; Magnusson, D.; Geist, A., Modified diglycolamides for grouped actinide separation. *J. Radioanal. Nucl. Chem.* **2017,** *314* (3), 2531–2538.

64. Wilden, A.; Kowalski, P. M.; Klaß, L.; Kraus, B.; Kreft, F.; Modolo, G.; Li, Y.; Rothe, J.; Dardenne, K.; Geist, A.; Leoncini, A.; Huskens, J.; Verboom, W., Unprecedented inversion of selectivity and extraordinary difference in the complexation of trivalent f elements by diastereomers of a methylated diglycolamide. *Chem. Eur. J.* **2019,** *25* (21), 5507–5513.

This project has received funding from the EURATOM research and training programme 2014–2018 under grant agreement No 730227